2009

The Role Of Adult Stem Cells And Tumor Necrosis Factor In Peripheral Neuropathy

Prabhjot Singh Dhadialla

Follow this and additional works at: http://digitalcommons.rockefeller.edu/
student_theses_and_dissertations

Part of the Life Sciences Commons

Recommended Citation

THE ROLE OF ADULT STEM CELLS AND TUMOR NECROSIS FACTOR IN

PERIPHERAL NEUROPATHY

A Thesis Presented to the Faculty of

The Rockefeller University

in Partial Fulfillment of the Requirements for

the degree of Doctor of Philosophy

by

Prabhjot Singh Dhadialla

June 2009

LOCATING THE THERAPEUTIC THRESHOLD OF FUNCTION IN PERIPHERAL NERVE DEVELOPMENT

Prabhjot Singh Dhadialla, Ph.D.

The Rockefeller University 2009

Peripheral neuropathies are a significant cause of morbidity and mortality, with a population prevalence of 2,400 per 100,000 (2.4%) that increases in the elderly to 8,000 per 100,000 (8%)(C. N. Martyn and R. A. Hughes, 1997). The variations in symptom distribution and etiologic attribution have resulted in the classification of over 100 types of peripheral neuropathy with specific patterns of development and prognoses. In the first study, we use a mouse model of hereditary peripheral neuropathy that results in hind-limb paralysis to investigate the therapeutic efficacy of adult, adipose derived stem cells (ADSC). The paralyzed mice that received ADSC transplantation demonstrated significantly improved motor function, likely due to stromal support provided by ADSCs. The ultrastructure of the nerve was not significantly improved, indicating that the threshold of functional motor improvement can be met through alternative means. In the second study, we developed a process to identify highly-connected genes in a model of peripheral nerve development using entropy maximized network analysis of gene microarrays. We found that Tumor Necrosis Factor (TNF) mediates axonal-Schwann cell communication, and that disruption of TNF signaling results in sensory and tissue dysfunction. These findings indicate that

the threshold of wild-type physiological function in peripheral nerve development

can be addressed by disrupting or strengthening specific signaling processes

without significant changes to tissue structure.

paataalaa paataal lakh aagaasaa aagaas

This thesis is dedicated to the communities who have shaped me in concert with

the warmth of my family.

ACKNOWLEDGEMENTS

TABLE OF CONTENTS

LIST OF FIGURES

LIST OF TABLES

CHAPTER 1

INTRODUCTION

1.1   Peripheral Neuropathies

Peripheral neuropathies are a significant cause of morbidity and mortality, with a

population prevalence of 2,400 per 100,000 (2.4%) that increases in the elderly

to 8,000 per 100,000 (8%)(C. N. Martyn and R. A. Hughes, 1997). Each

peripheral nerve has a specialized function that must be relayed to the brain and

spinal chord, resulting in a wide array of symptoms when they are damaged.

These constellations of symptoms are the effects that people usual feel when

they contact a doctor for diagnosis. Because peripheral nerves can carry both

motor and sensory information, people may experience symptoms ranging from

temporary numbness, sensitivity and muscle weakness to burning pain, muscle

wasting, paralysis and organ dysfunction. These symptoms can be isolated to

one nerve (mononeuropathy), multiple physically related nerves (polyneuropathy)

or multiple physically unrelated nerves (mononeuritis multiplex). The variations in

symptom distribution and etiologic attribution have resulted in the classification of

over 100 types of peripheral neuropathy with different histories of development

and prognoses. Although there is considerable overlap in patterns of disease

progression, there is no common framework for treating or investigating

peripheral neuropathies.

Peripheral neuropathies can be acquired through systemic disease, trauma environmental wear, infections or autoimmune processes. In addition, there are clearly defined inherited peripheral neuropathies such as Charcot-Marie-Tooth syndrome and Merosin-Deficient Muscular Dystrophy, which are characterized by gait abnormalities, wasting of muscles in the lower legs and feet and numbness in the lower limbs (K. Matsumura et al., 1997; M. L. Feltri and L. Wrabetz, 2005; Y. Parman, 2007). In many cases, inherited defects remain sub-clinical until environmental damage through the acquired pathways listed above result in clinical presentation. The interaction between inherited and acquired peripheral neuropathies has not been well described. To date, there are no medical treatments to cure an inherited peripheral neuropathy. Thus far, therapeutic approaches for the vast majority of peripheral neuropathies have been limited to amelioration of symptoms through nutritional support, physical rehabilitation and general immunosuppressive therapy (R. A. Hughes, 2002).

The underlying etiology varies according to cell type and function targeted by the disease process. For many neuropathies, nerve dysfunction results from Schwann cell defects. Schwann cells not only insulate axons, but also maintain their long-term functional integrity. Loss of glial support results in progressive axon degeneration and local inflammation, contributing to the development of peripheral neuropathies (K. A. Nave and B. D. Trapp, 2008). Although difficult to disambiguate entirely, doctors classify peripheral neuropathies as predominantly

motor, predominantly sensory, sensory-motor or autonomic; classification is related to the type of Schwann cell-axon interaction involved.

1.2. Schwann Cell Development and Neuropathy

Schwann cells differentiate from the neural crest, and as they mature, sort axons by inserting cytoplasmic protrusions between axons until no unsheathed axons remain (R. Mirsky and K. R. Jessen, 1996; R. Mirsky et al., 1996; K. R. Jessen and R. Mirsky, 1997). Schwann cells can either myelinate one axon or envelop multiple axons with their cytoplasm in order to provide insulation and environmental support (**Figure 1)**.
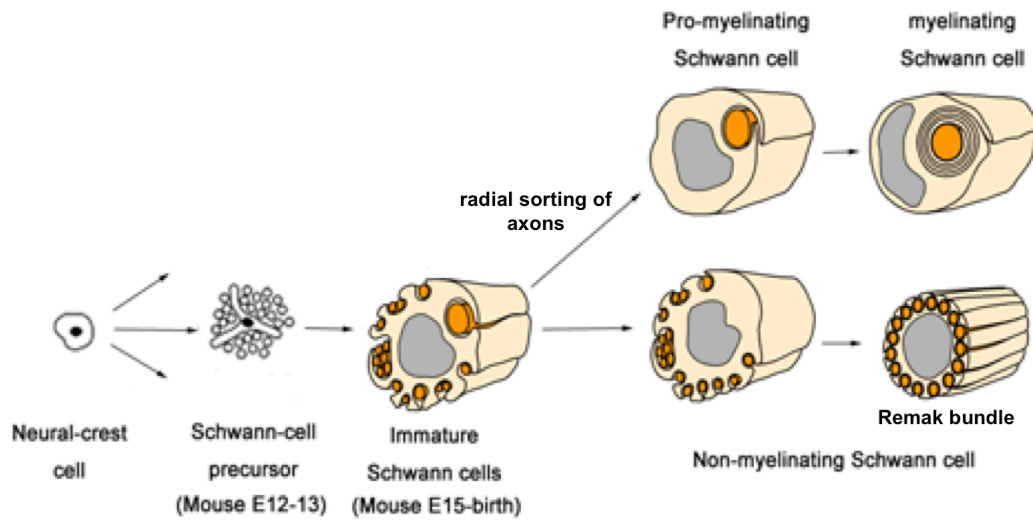
Figure 1. The mouse Schwann-cell lineage (modified from Jessen and Mirsky, 1999b; Basic Neurochemistry, 6th Ed, 1999, Fig 27-16).

The myelin sheath forms as multiple layers of Schwann cell membrane enwrap a single axon. Myelination of axons is essential for proper function of the nervous system, predominantly because it allows for the fast conduction of action potentials.   Myelination of the peripheral nervous system (PNS) is accomplished by Schwann cells, the major glial cells of the vertebrate PNS. During embryonic development, Schwann cell precursors are derived from the neural crest, which occurs at embryonic day (e) 12-13 in the mouse. The survival of Schwann cell precursors is dependent on axon-derived signals (K. R. Jessen and R. Mirsky, 2002; R. Mirsky et al., 2002). When immature Schwann cells are generated from Schwann cell precursors (e13-15 for mouse), they lose this axon dependence and support their own survival by establishing autocrine loops (K. R. Jessen and R. Mirsky, 2005). At this time, some Schwann cells destined to myelinate will proliferate vigorously and differentiate into promyelinating Schwann cells, from which individual cells extend their cytoplasmic processes into bundles of axons, progressively separate them into even smaller bundles, and finally establish a 1:1 relationship with each larger diameter axon, a process known as radial sorting (H. D. Webster, 1993). These cells will further differentiate and wrap axons concentrically with the extension of their membrane and produce myelin sheaths (myelinating Schwann cells). Non-myelinating Schwann cells appear late in the PNS, at approximately P15-20, and they can only envelop a definite number of small caliber axons (5~30 axons) (E. J. Arroyo et al., 1998). Development of myelinating Schwann cells precedes nonmyelinating Schwann cells, and

nonmyelinating Schwann cells enwrap multiple small caliber axons only after the

myelinating Schwann cells reach a 1:1 ratio with individual large axons (P. A.

Eccleston et al., 1987). Nonmyelinating Schwann cells envelop multiple small

caliber axons (C fibers, <1 μm diameter) to form a Remak bundle and keep

individual axons separated by membrane extensions, but they do not form myelin

sheaths(K. R. Jessen and R. Mirsky, 2005). Remak bundles convey sensory

information along the peripheral nerve bundle (**Figure 2**)

Disruption of myelinating Schwann cell development results in peripheral motor

neuropathies. Mutations in laminin α2 cause Merosin Deficient Congenital

Muscular Dystrophy in humans (CMD1A), which is the most common type of

congenital muscular dystrophy (A. Helbling-Leclerc et al., 1995). Studies from

mice and Dorsal Root Ganglia co-cultures lacking the laminin family of genes in

Schwann cells provide extensive evidence that laminins play multiple essential

roles during the various aspects of PNS development. These include the

proliferation, survival, and differentiation of Schwann cells. In CMD1A patients,

both muscle and peripheral nerves are affected, and the phenotypes are a

combination of nerve and muscular pathology, including progressive hind limb

paralysis due to peripheral nerve hypomyelination (W. Kuang et al., 1998). This

suggests that deficiency of Schwann cell laminins contribute to the pathogenesis

of peripheral nerve neuropathy. In addition to CMD1A, mutations of laminin

signaling components also contributes to the pathogenesis of other heritable

peripheral neuropathies such as Charcot-Marie-Tooth 4F (mutations in *periaxin*

gene) and neurofibromatosis (mutation in *NF2/schwannomin* gene) (M. L. Feltri and L. Wrabetz, 2005). The disruption of laminins compromises the ability of myelinating Schwann cells to provide structural and signaling support to axons.
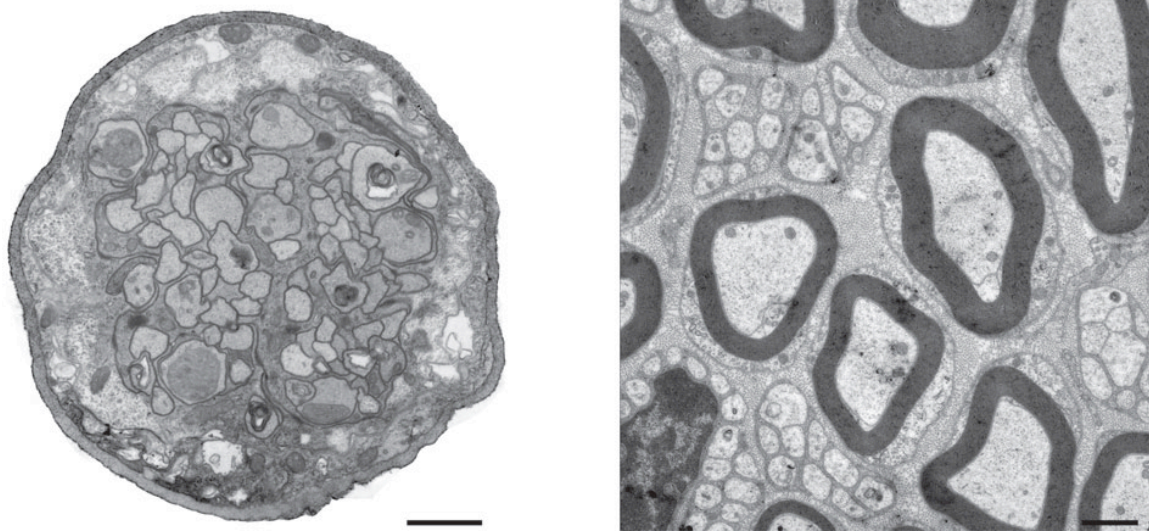
Figure 2. Peripheral Nerve Structure. Electron micrograph of a peripheral nerve showing glial cell processes that interdigitate and envelop single axons (*left*). The relationship is similar to that of nonmyelin-forming Schwann cells that envelop small-caliber C-fiber axons in the mouse sciatic nerve (*right*). Scale bar, 1 μm.(K. A. Nave and B. D. Trapp, 2008)

Schwann cells have a well-defined role in peripheral nerve tissue homeostasis in times of disease beyond the structural features of myelin formation and axon insulation. It has been recognized that Schwann cells are immunocompetent, and can modify the peripheral nerve tissue environment through immunomodulation of local cytokines. Schwann cells can produce and secrete a range of cytokines, including Interleukin-6, transforming growth factor β, and Tumor Necrosis Factor (TNF)α (K. Bergsteinsdottir et al., 1991; G. Stoll et al., 1993; O. Bourde et al., 1996) (**Figure 3)**. Previous studies have shown that TNF is expressed in Schwann cell cytoplasm (C. Cheng et al., 2007) in an autocrine and local paracrine fashion (Y. Qin et al., 2008) can directly modulate synaptic scaling in the spinal chord(D. Stellwagen and R. C. Malenka, 2006). Some cytokine receptors, such as TNF Receptor 1 (TNFR1) are constitutively expressed on Schwann cells, facilitating a TNFα response (B. Bonetti et al., 2000). The role of these components has been extensively explored during the course of inflammatory neuropathies as well as non-inflammatory hereditary neuropathies (G. Meyer zu Horste et al., 2008). In addition, nuclear transcription factor-κB (NFκB), a traditional regulator of cytokines, is activated in human Schwann cells (R. M. Pereira et al., 2005). The natural inhibitor of NFκB, IκB, it abundantly present in Schwann cells, indicating an active rather than passive role for NFκB in peripheral nerve physiology (B. Andorfer et al., 2001). Anti-inflammatory treatment of non-inflammatory hereditary neuropathies such as Charcot-Marie-Tooth disease has been controversial, as the suppression of one neuropathy can
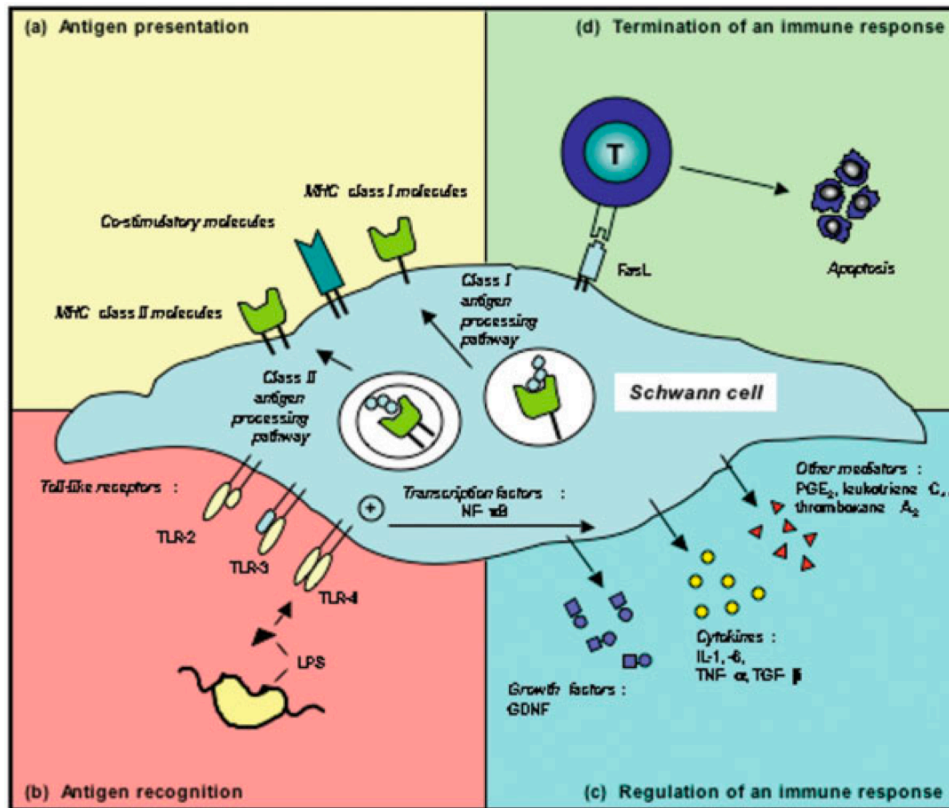
Figure 3. Immunocompetence of Schwann cells. (a) Schwann cells can express the major histocompatibility (MHC) class I molecules as well as MHC class II molecules along with co-stimulatory molecules (b) Schwann cells can recognize antigens via Toll receptors, such as LPS, activating the nuclear transcription factor NF-κB. (c) Schwann cells regulate the immune response post-stimulation by secreting soluble factors like cytokines, growth factors, and other immune mediators. (d) Schwann cells terminate the immune response via the interaction of Fas and FasL, triggering apoptosis in inflammatory T cells. *LPS, lipopolysaccharide; GDNF, glial cell line– derived neurotrophic factor; PGE2, prostaglandin E2; IL, interleukin; TNF, tumor necrosis factor; TGF, transforming growth factor.* (Adapted from (G. Meyer zu Horste et al., 2008)

lead to the development of a new one in the form of sensory loss or

dysmyelination (M. Berghoff et al., 2005). The ambiguous role of cytokines in

normal Schwann physiology is highlighted by the emergence of sensory

neuropathies during systemic administration of TNFα for a range of unrelated

conditions (C. Sommer et al., 2001; J. P. Stubgen, 2008). Although this has been

largely attributed to the sequelae of an immune response, an alternative

hypothesis is that nervous system tissues that use these molecules for

communication are disrupted (M. Empl et al., 2001; J. C. Czeschik et al., 2008).

Indeed, these hypotheses are not mutually exclusive. It has been difficult to

disambiguate the primary role of cytokines in disease processes from secondary

immune responses. After stimulation with proinflammatory cytokines, FasL (a

member of the TNF family) can interact with T-Cells to promote apoptosis,

suggesting that Schwann cells may also have a role in terminating secondary

immune responses.

1.3 Adult Stem Cells and Therapeutic Potential

Stem cells can serve as a source of cells to repopulate injured tissues, produce

molecules that provide a supportive environment for endogenous tissue, and

may be useful as renewable biological delivery vectors for targeted gene therapy.

The design of stem cell therapy is heavily influenced by the type of stem cell

used for transplant. Embryonic Stem Cells (ESCs) are the earliest non-germ

stem cell line, and offer the widest potential of cell types in tissue repair. ESCs become increasingly differentiated over time, developing towards ectodermal (including neural crest lineage tissues), endodermal or mesenchymal fates. However, because of the wide range of cell types that they may generate, several animal studies of transplanted ESCs have resulted in teratoma-type malignancy generation, which may limit ESCs therapeutic usefulness. One avenue that investigators have employed to circumvent teratoma formation is to push ESCs towards a tissue-specific lineage. Neural precursor cells and dopaminergic neurons have been generated from ESCs, and it has been shown that these cell lines can migrate and further differentiate into appropriate neuronal cell types in the rodent CNS (A. L. Perrier et al., 2004). This same group has recently developed methodologies to generate neural crest stem cells from ESCs (G. Lee et al., 2007). Newly derived neural crest stem cells may afford a unique opportunity to repopulate developmentally aberrant peripheral nerves in a tissue-appropriate manner.

The relatively restricted fates of adult stem cells make these populations a potential alternative when applied to appropriate tissue environments. In the adult animal, there are populations of stem cells that can be isolated from a variety of tissues. Although generally more fate committed than embryonic-type stem cells, mesenchymal stem cells in particular are multipotent, with the potential to give rise to many non-mesenchymal cell types, including Schwann cells and neurons. Adipose tissue is a readily available source of mesenchymal

stem cells, termed Adipose Derived Stem Cells (ADSCs). ADSCs are easily

isolated from adipose tissue, and can be maintained in culture through at least

eight cell passages. Mesenchymal stem cell lines such as ADSCs have the

added advantage of being relatively immune-privileged. These cells have been

shown to differentiate into a number of cell types including bone, cartilage,

muscle, adipose and stromal support cells (**Figure 4**). They do not express

major histocompatibility antigen (MHC) class I molecules on their cell surface and

thus do not elicit significant immune reaction when transplanted into even

unrelated animal species. For instance, ADSCs derived from human lipoaspirate

have been used to seed skeletal muscle in dystrophin knockout mice for

extended periods of time. Transplants are maintained without the necessity for

immunosuppressant therapy. ADSCs offer the advantage of easy accessibility,

multipotency and immune privilege status, although the longevity and

functionality of transplant is not yet established.

www.cytoritx.com/ stemcell/images.htm

White Adipose

FAT

Collagenase

200g X 10 minutes

Adipocytes

Pellted Stem Cells

Adipose Stem Cells

Bone   Cartilage   Adipose   Muscle   Nerve/Schwann?
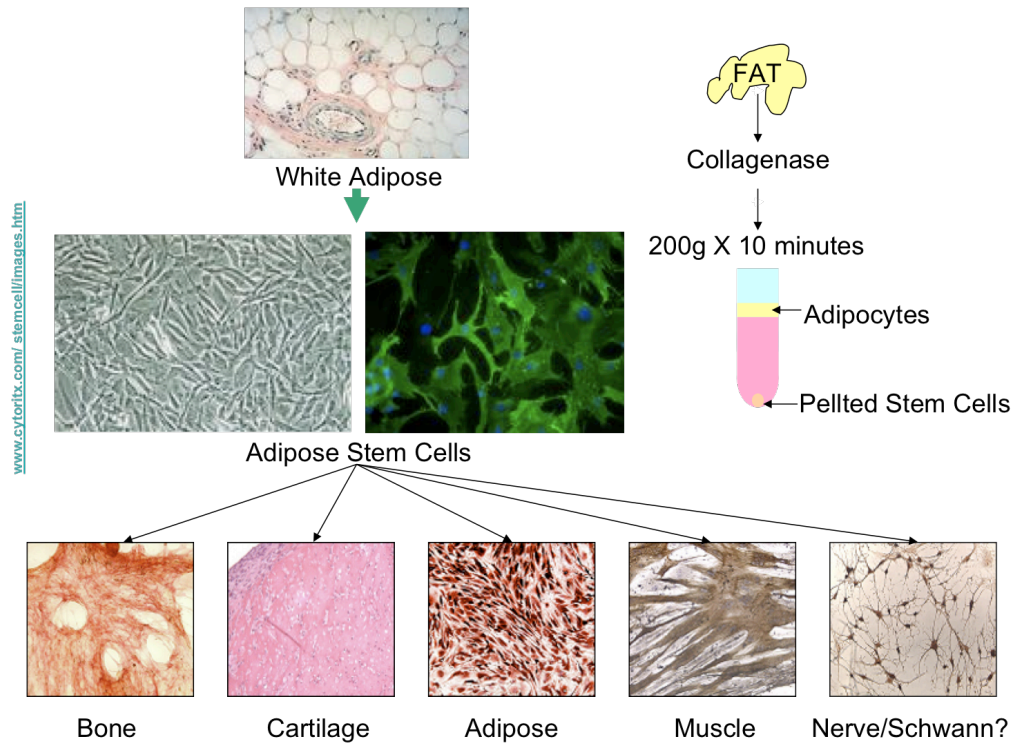
Figure 4. Differentiation of ADSCs. White adipose is separated into Adipocytes and stem cells. The stem cells can be further differentiation into bone, cartilage, adipose and muscle. Nerve/Schwann cell lineages have been reported. (Adapted by Karen B. Carlson from *Cytotrix*)

Several studies have examined the potential for transplanted stem cells to repopulate injured peripheral nerves. In a model of chronic denervation, neural stem cells could improve electrophysiologic function of the injured nerve and be engineered to supply supportive factors such as GDNF (Glial Derived Neurotrophic Factor) to targeted tissues (G. Stoll and H. W. Muller, 1999). Adult hair follicle stem cells, a non-neuronal adult multipotent stem cell line, have also been used to support repair in transected sciatic nerves (Y. Amoh et al., 2005). The non-neuronal stem cells repopulated the injured nerve with myelinating Schwann cells and subsequently restored hind limb function according to gross functional measurements.

Stem cell transplant strategies have been explored for many tissue types, including injured neuronal tissues. However, transplant into models of heritable peripheral neuropathies such as CMD1A in which glial development is arrested have not been explored. Similarly, the molecular mechanisms by which stem cells impact the PNS microenvironment, and by which the PNS microenvironment impacts transplanted stem cells have also not been determined. Efforts to understand the gene interactions that orchestrate the nerve tissue microenvironment during development are crucial to improving the therapeutic potential of stem cells.

1.4 Maximum Entropy Analysis of Gene Microarray

As the density of genetic regulatory information increases, so does the importance of identifying pivotal molecules that regulate complex processes such as peripheral nerve development. Perturbation of these molecules provides insight into the relationship between development processes and therapeutic possibilities for peripheral neuropathies. Gene microarray analysis has been successfully used to identify crucial molecular components of genetic systems. The magnitude of gene expression is commonly inferred from microarray analysis of tissues using computational methods. A variety of grouping techniques, such as cluster analysis, Bayesian statistics, independent component analysis (ICA), principle component analysis (PCA) and network component analysis (NCA) are employed to categorize transcriptional profiles from microarrays while assuming steady state conditions (N. S. Holter et al., 2000; N. S. Holter et al., 2001; F. Azuaje, 2002; W. Liebermeister, 2002; W. Pan, 2002; I. Shmulevich et al., 2002; J. C. Liao et al., 2003; N. Bolshakova and F. Azuaje, 2006). Time delayed, complex relationships that are further complicated by measurement noise are difficult to capture within the parameters of these methods. Nevertheless, these groupings can be useful because proteins encoded by genes in biological processes are often co-regulated. Although useful to understand aggregate patterns, they provide little insight into inferred gene network interactions (P. D'Haeseleer et al., 2000; P. D'Haeseleer, 2005).

Linear models of gene network interactions are particularly sensitive to undersampled datasets, because poor parametric assumptions are amplified as the underdetermination increases (J. Tegner et al., 2003; S. Li et al., 2006). This is particularly accentuated in expression data captured over time-series, where only a few time points may be all that are available to parse arrays of thousands of genes measured in parallel into biologically useful gene interaction network models. Boolean networks of cellular processes, Bayesian network models, relevance networks and those predicated upon particular underlying statistical distributions create constraining assumptions about the nature of the network from the outset (S. Liang et al., 1998; T. Akutsu et al., 2000; N. Friedman et al., 2000; N. Friedman, 2004). Enriching networks with qualitative information from systematic literature mining, as well as targeted experiments becomes difficult as the number of with genes and possible network configurations increase (T. Ideker et al., 2001; J. Tegner et al., 2003).

Maximum entropy analysis of gene arrays takes a different approach to the problem of undetermination in large data sets. This approach is based upon Boltzmann's concept of entropy maximization, which supports statistical inference with minimal reliance on missing information. In this analysis, a given biological process is considered a macroscopic state composed of microscopic states (i.e. gene expression). Since there are many possible configurations of microscopic states that could result in the macroscopic state, the state that

17

corresponds to the largest number of correlated microscopic states is most likely.
Since information and entropy, as defined by Shannon, are inversely related, the
network selected by the entropy maximizing procedure has the least reliance on
missing information (C. E. Shannon, 1997). This procedure is predicated upon
constructing a network topology from pairwise interactions that use the least
information (maximizing entropy) to empirically explain the resulting
transcriptional profile. Any alternative network state would lower the entropy of
the entire system, by requiring missing information. Entropy maximization
analysis has been used to successfully represent complex interactions in diverse
nonequilibrium systems including genetic and neural networks based upon
pairwise interactions (T. R. Lezon et al., 2006; E. Schneidman et al., 2006; A.
Sayyed-Ahmad et al., 2007). This approach is not free of assumptions: the use
of mRNA transcription levels rather than a comprehensive cell model is
dependent upon tight overall relationships between the genome, proteome and
metabalome.

1.5 Genetic Network Maps and Target Prioritization

Biological network visualization focuses on the interplay between individual
genes and apparent sub-groups. This tool does not require detailed quantitative
descriptions of subsystem dynamics in order to suggest information about gene
function and the potential impact of transcriptional loss (N. Yeung et al., 2008).

The trade-off is that a network map is indicative rather than predictive for pertinent interactions between biological components. A systematic approach to target prioritization is required to make use of these maps in resource-limited experimental contexts.

Gene networks are usually represented as graphs in the form of nodes (genes or gene products) and edges (interactions). Since the magnitudes of interactions are rarely captured in this form, the general structure/topology of networks has received more attention. As reviewed by Khanin and Wit, biological networks (gene – *g-space*, protein *p-space*, and metabolic – *m-space*) have largely shown the following characteristics: 1) each node is connected to other systemic nodes through a short path (*small world topology*), 2) there are many nodes with few connections and a few nodes with many connections (*hubs)*, and 3) hubs are enriched with essential/lethal genes (*centrality/lethality*) (R. Khanin and E. Wit, 2006) (**Figure 5**). Previous studies have indicated that metabolic, protein and genetic networks appear to be scale-invariant and follow power laws, such that relationship between genes and the number of linkages to other genes in the network increased logarithmically (A. Rzhetsky and S. M. Gomez, 2001; D. E. Featherstone and K. Broadie, 2002; E. Ravasz et al., 2002; A. L. Barabasi and Z. N. Oltvai, 2004; V. van Noort et al., 2004; A. Fernandez, 2007). This property is attractive in biological systems because scale-free networks allow for fast communication and resistance to breakdown (E. Almaas et al., 2005). Further

careful study of these same and related biological networks has shown that they are rarely truly scale-free, although some of the major features of scale-free networks are present (E. Alm and A. P. Arkin, 2003; R. Khanin and E. Wit, 2006). Nevertheless, the number of connections per node in a network in an important way of parsing network topographies for genes with potential functional relevance to the biological process described by microarray data (D. S. Lee et al., 2008). Genes with a high number of connections per node and demonstrated physiological relevance are termed "influential." These network maps provide useful starting points for experimental exploration of influential genes. Gene interactions in a simple tissue system, such as those between Schwann cells and neurons undergoing peripheral nerve development, have not yet been explored.
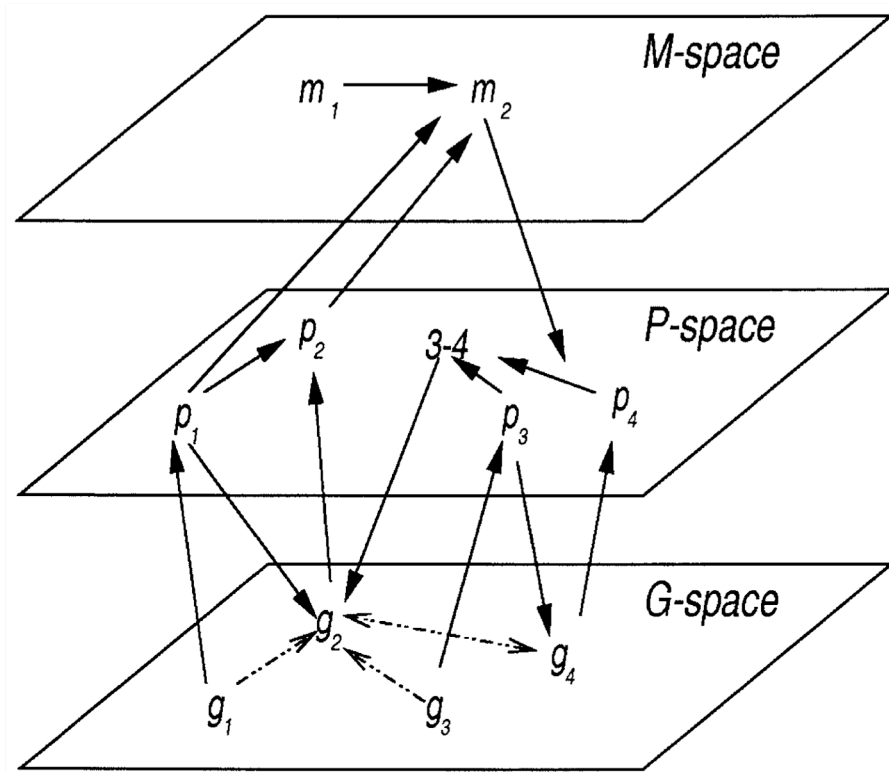
Figure 5. Cellular Biological Networks. This representation of cellular biological networks includes closely interconnected and interrelated spaces. Here G-space stands for a space of gene interactions, P -space is a space of protein interactions, and M-space is a space of interactions between metabolites. Solid arrows represent direct causal interactions, whereas the dotted arrows are indirect gene interactions, which occur via intermediate causal interaction(s). All three types of networks have been previously studied using a graph approach, and they have all been shown to share certain characteristics, such as small-world property and existence of hubs with a high proportion of essential/ lethal nodes. (Adapted from (R. Khanin and E. Wit, 2006).

1.6 Objectives

Peripheral neuropathies represent a heterogeneous group of pathologies that present with a constellation of overlapping symptoms. Despite common effects on nervous tissue, broad classes of common mechanisms have not been identified. As a result, current therapeutic avenues address the symptoms of peripheral neuropathies rather than the underlying cause. Therefore, new therapeutic options and means of identifying influential genes in peripheral nerve development and function are crucial. We seek to use stem cell therapeutics and analytic tools to find influential genes with functional relevance to a disease model and normal process of peripheral nerve development, respectively.

CHAPTER 2

MATERIALS AND METHODS

2.1 Mice

Mice were maintained in the Rockefeller University Laboratory Animal Research Center (LARC) and treated in accordance with protocols approved by LARC. All experiments involving animals was performed with the approval of the Institutional Animal Care and Use Committees. The Wildtype mice C57/BL6 background) were obtained from Jackson Laboratory (Bar Harbor, ME). The *Laminin-γ1 Mice* were generated through a knockout approach. To knock out laminin-γ1 in Schwann cells, mice in which Cre expression is under the control of the Schwann cell specific- myelin P0 promoter (M. L. Feltri et al., 1999) were crossed with mice in which the laminin γ1 gene is flanked by LoxP sites (fLamγ1 allele) (Z. L. Chen and S. Strickland, 2003; W. M. Yu et al., 2005). Mice were genotyped by PCR for both the Cre transgene and homozygosity of the fLamγ1 allele. Mutant (P0Lamγ1-/-) mice were homozygous for the fLAMγ1 allele and carry one copy of the P0-Cre transgene. Mice used as controls in these experiments were heterozygous for both the fLAMγ1 allele (Lamγ1f/+) and the P0-Cre transgene (hereafter referred to as control mice). The Tumor Necrosis Factor -/- mice were obtained from Jackson Laboratory (Bar Harbor, ME). They

were generated by deleting 40 base pairs of the 5' UTR, all the coding region, including the ATG translation initiation codon of the first exon and part of the first intron of the muTNFa gene. All mice used in this study were bred on a C57/BL6 background for at least 5 generations.

2.2 Stem cell culture and verification

ADSCs were isolated according to a standard technique as follows (S. H. Gee et al., 1993; L. Y. Yang et al., 2004; Y. S. Choi et al., 2006): peri-inguinal fat pads were removed from adult mice and rinsed twice with sterile PBS (Gibco-Invitrogen; Carlsbad, CA). Fat pads were then placed in DMEM (Gibco-Invitrogen; Carlsbad, CA) containing Pen-Strep antibiotics (Sigma; St. Louis, MO), 2mg/mL collagenase (Sigma; St. Lous, MO), and 1% BSA (Gibco-Invitrogen; Carlsbad, CA), minced, and digested with agitation at 37°C for 45 minutes. Tissue homogenate was then treated with FBS (Gibco-Invitrogen; Carlsbad, CA), and centrifuged at 200g x 4 minutes. The supernatant containing adipocytes was discarded, and the stromal-vascular pellet was resuspended in DMEM with 10% FCS and antibiotics. The resulting cell suspension was then filtered through a 70 micron filter and plated at a density of 10,000 cells/cm2. Cultures were grown to approximately 80% confluence prior to subculturing. Cell cultures were used between passage 2 and 5. Identity of ADSCs was initially

verified by flow cytometry for Thy1, CD44, and CD49b (98%, 95%, 92%

respectively) as has been previously described (A. M. Rodriguez et al., 2005).

The 3T3/L1 cells (ATCC; Manassas, VA) were grown as described previously in

DMEM containing 10% FBS and antibiotics (S. J. Yarwood and J. R. Woodgett,

2001).

2.3 Stem cell transplant

Adult mutant mice were anesthetized, and sciatic nerves were surgically exposed

using aseptic surgical techniques. Cells (ADSC or 3T3/L1) suspended (J.

Fujimura et al., 2005) in 20-40 μl of culture media or murine laminin-1 (23 μg;

Sigma ;St. Louis, MO) were pipetted onto the indicated nerve. The contralateral

nerve received an equivalent volume of media without cells. Surgical wounds

were then closed with a 5-O SofSilk suture and vet-bond tissue adhesive (3M;

Minneapolis, MN). Images, tissue samples and electrophysiological recordings

were collected seven to 21 days post-injection as indicated in each figure.

2.4 Electrophysiology

There is some variance between mutant mice with respect to the severity of hindlimb phenotype. Therefore, comparisons were always made between limbs of the same mouse. Electrophysiologic analysis showed minimal variance between limbs of the same mutant mouse. Electrophysiological measurements were made using standard stimulating and recording methods. Mice were anesthetized with an avertine/atropine mixture and placed on a plexiglass platform affixed to a stereotaxic apparatus. Sciatic nerves were surgically exposed, and a blunt tip stimulating electrode was placed on the proximal sciatic nerve. A recording electrode was then inserted into the muscle with the observed twitch. Constant current pulses (0.15msec duration; 10-1000 μA) were administered and recordings were collected from the resultant evoked potential. The amplitude of each potential was calculated as the amplitude between the start of the positive deflection and maximum amplitude. The nerve conduction latency (NCL) was calculated by dividing the length of time between stimulus onset and start of evoked potential by the distance between stimulating and recording electrodes. Each measurement was made three times and averaged.

2.5 Electron Microscopy

Seven days after stem cell/ media transplant, sciatic nerves were collected and fixed in 2.5% paraformaldehyde/ glutaraldehyde and 2% osmium tetroxide

solution (Electron Microscopy Sciences; Hatfield, PA)(Z. L. Chen and S.

Strickland, 2003; W. M. Yu et al., 2005). Nerves were prepared, embedded in

resin, cut into ultra-thin sections, and visualized by electron microscopy as

previously described (Z. L. Chen and S. Strickland, 2003; W. M. Yu et al., 2005).

Electron micrographs of DRG-co cultures were obtained by scraping the fixed

monolayer intact, creating a pellet that does not disrupt cell interactions, and

transecting it to obtain a random sampling of the DRG co-culture.

2.6 Immunostaining

Seven to 21 days post-transplant, mice were anesthetized with 2.5% avertine

solution and transcardially perfused with PBS followed by 2.5%

paraformaldehyde. Sciatic nerves were removed and post-fixed overnight in the

same solution. Tissues were cryoprotected in 30% sucrose solution for two days

prior to sectioning. Nerves were sectioned into 10 μm intervals using a Leica

cryostat, and sections were adhered to superfrost plus glass slides (Fisher

Scientific) (Z. L. Chen and S. Strickland, 2003; W. M. Yu et al., 2005). Cell

cultures were grown on Poly-D-lysine-coated coverslips (BD Biosciences; San

Jose, CA) and then processed in the same manner as tissue samples detailed

below. Tissue and cell samples were processed for immunofluoresence by

fixation in 4% paraformaldehyde for 20 minutes followed by thorough rinsing in

PBS. Samples were blocked in PBS containing 5% normal goat serum for one

hour. Samples were incubated overnight at 4 °C with primary antibodies (1:500

for MBP, Chemicon; Temecula, CA; or 1:1,000 for laminin-1, Sigma; St. Louis,

MO). After thorough rinsing in PBS, secondary antibodies (1:1000 for Alexa 488-

labeled anti-rat and Alexa 488-labeled anti-rabbit IgG; Invitrogen; Eugene, OR)

were applied for one hour at room temperature. Samples were then well rinsed

and visualized using a Zeiss LSM 510 confocal microscope at The Rockefeller

University Bio-Imaging Resource Center.

2.7 DRG co-culture and associated reagents

Wild type mice are obtained at E13.5 for the extraction of dorsal root ganglia

(DRG), which contain two main cell populations, Schwann cells and neurons.

The DRG is disassociated and maintained until a dense layer of Schwann cells

exists in tight proximity to neurons (-9 days). The onset of Schwann cell-axonal

maturation was triggered by adding ascorbic acid, defining time point zero as

previously described (Z. L. Chen et al., 2008). Samples for microarray analysis

were obtained in triplicate from separate co-culture slips at 0, ½, 1, 6, 12, 36 and

48 hours post ascorbic acid addition and prepared for use on Illumina Mouse-8

chips (Illumina, Inc.) by the Rockefeller Microarray Core Facility. Co-culture for

EM analysis were obtained at day +9. aTNF neutralizing antibody (Abcam) was

administered to co-cultures at saturating concentrations (reported ND_{50}=0.08-0.1

28

ug/ml; 1ug/ml used). A polyclonal IgG control (Abcam) was used at the same

concentration. rmTNF (R&D Systems) was prepared at the following

concentrations: 5ng/ml, 0.5 ng/ml, 0.5 ng/ml and 0.05 ng/ml.

2.8 Maximum Entropy Analysis and Network Mapping

For microarray data, the expression levels of genes, at time t, can be considered

to be a vector, x, of n genes. Sampling gene expression levels at different times

leads to a distribution over these vectors, which describes the behavior of the

network. One simplification is to assume that the behavior of the network is

determined completely by interactions between pairs of genes and not by any

higher interactions (such as interactions between triplets). As shown by Lezon et

al., the matrix of interaction strengths M between genes is simply the inverse of

the covariance matrix of the expression levels of these genes(T. R. Lezon et al.,

2006).

The raw expression data was normalized and averaged using Illumina software.

Further analyses were performed using custom software written in Matlab

(Natick, MA). Genes were selected that are reliably detected at all time points

with a detection p-value greater than 0.9. Expression levels for each gene were

rendered relative to baseline by subtracting out expression levels at time 0. Then

n genes (typically 200-500) were selected that had the highest variance

expression levels over the course of the experiment. This formed an N-by-t array,

X, of n genes, sampled at t times. The covariance matrix of this array C_{ij} was

calculated, which describes the variance of each gene i with every other gene j.

Since this matrix is generally noninvertible, the pseudoinverse, M_{ij}, which

contains the interaction strengths for each gene i with every other gene j was

calculated. To determine which genes have a significant interaction, a threshold

for interaction strengths was established: interactions which are 2 or 3 standard

deviations above (or below) the mean were counted as positive (or negative)

interactions (**Figure 6)**.
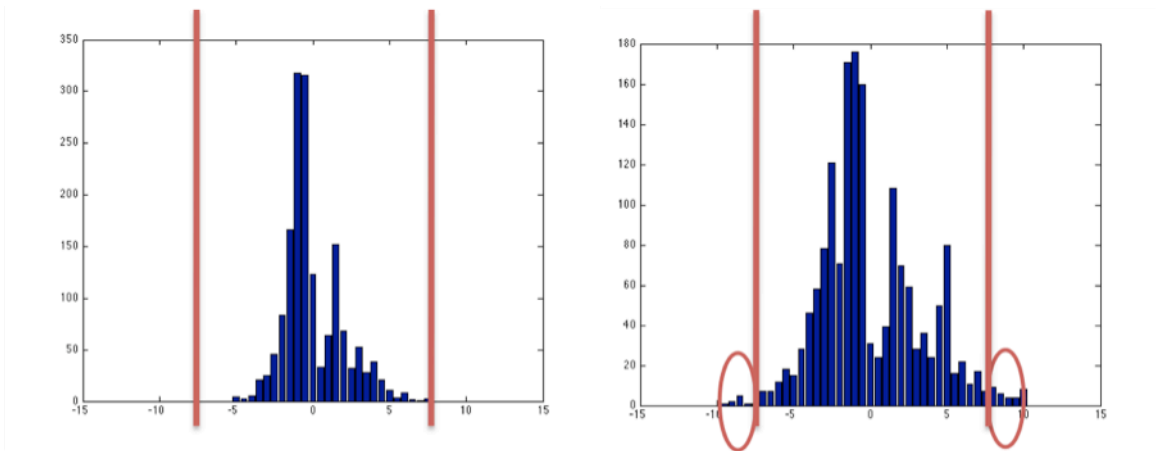
Figure 6. Determination of covariance factor cutoff. A covariance factor is calculated for all gene profiles in relation to all other included gene profiles (500 genes). This results in an individual gene profile like those represented, with the center representing the number of included genes with no covariance factor, positive values representing temporal gene profiles with correlated covariance factors and negative values representing anti-correlation. The magnitude of this value indicates the strength of the covariance factor, and the overall distribution of each gene profile allows a standard deviation cutoff from baseline to be user-defined, resulting in a variable size network based upon this value (2 or 3 standard deviations were chosen in this study). The figure on the left depicts a vertical red bar representing a standard deviation cutoff that does not admit any genes that should be included as "connected" to this gene, while the figure on the right depicts cutoff values that admit multiple connections.

The commented Matlab code is displayed below:

```
%%
% Remove data with pvalues<0.10
[not_detectedI]=find(DataPVal<=0.05);

DataAvg(not_detectedI)=0;

% Find no mRNA signal for all time points
colSum=sum(DataAvg,2);

GenesNotExpressed=find(colSum==0);

size(GenesNotExpressed);

GenesExpressed=find(abs(colSum)>0);

%Throw out not expressed genes
DataAvg=DataAvg(GenesExpressed,:);

DataPVal=DataPVal(GenesExpressed,:);

GeneName=GeneName(GenesExpressed);

GeneDefinition=GeneDefinition(GenesExpressed);

GeneTargetID=GeneTargetID(GenesExpressed);

%Keep only genes expressed at all timepoints
[findzerosI,findzerosJ]=find(DataAvg==0);

rows2keep=setxor(findzerosI,[1:size(DataAvg,1)]);

DataAvg=DataAvg(rows2keep,:);

GeneName=GeneName(rows2keep);

GeneTargetID=GeneTargetID(rows2keep);

GeneDefinition=GeneDefinition(rows2keep);

DataVar=DataAvg-repmat(DataAvg(:,1),1,8);

DataVar=var(DataAvg,0,2);

%VarList=sort(DataVar);

DataVar=[DataVar (1:length(DataVar))'];

VarList=sortrows(DataVar,1);

VarList=flipud(VarList);

VarList=VarList(1:200,:); %For a larger network, increase this to >200, but it will run slower

DataKeep=zeros(length(VarList),size(DataAvg,2));

for i=1:length(VarList)

    index=VarList(i,2);
```

```
    DataKeep(i,:)=DataAvg(index,:);

    GeneDefinitionKeep(i)=GeneDefinition(index);

    GeneTargetIDKeep(i)=GeneTargetID(index);

    GeneNameKeep(i)=GeneName(index);

end

%%
```

The network was visualized using Cytoscape software (National Institutes of Health) using spring-embedded and degree-weighted views without considering the directionality of interactions.

2.9 Motor and Sensory Function Testing

There is some variance between mutant mice with respect to the severity of hindlimb phenotype. Therefore, comparisons were always made between limbs of the same mouse. Changes in hind-limb function following cell-treatment were measured by determining the minimum current needed to produce an observable muscle twitch (MCST). MCST function-testing showed minimal variance between limbs of the same mutant mouse (data not shown). Mice were anesthetized with an avertine/atropine mixture and placed on a plexiglass platform affixed to a stereotaxic apparatus. Sciatic nerves were surgically exposed, and a blunt tip stimulating electrode was placed on the proximal sciatic nerve. Minimum current needed to produce a muscle twitch (MCST) was determined by applying 0.15msec current pulses starting at 100 μA and successively increasing the

amplitude until a twitch was detected. Exposed muscle was observed under a

dissecting microscope for evidence of muscle twitch. This technique was

performed in triplicate for each nerve. Motor ability was also assessed using the

accelerating Rotarod (IITC Life Science, California) from each group of wild type

and TNF-/- mice (F. Prestori et al., 2008). Sensory function was assessed by

determining the latency (sec) to jump or lick the front or hind paws after being

placed on a 52°C hot plate.

2.10 Image and Statistical Analysis

Electron Microscope Image Analysis

Electron micrographs of 21 day old male WT and TNF-/- mice were obtained for

sciatic nerve analysis. Axon size variation was measured from digital electron

micrographs of sciatic nerves using ImageJ (National Institutes of Health). Axon

juxtaposition and envelopment was determined by consistently applying a metric

of <60%=juxtaposition and >60%=envelopment to Schwann cell cytoplasmic

envelopment of axons where all cells have intact borders as viewed on the

transecting field.

Statistical Analysis

All values are expressed as mean and standard deviation (s.d.) as indicated. Analyses of significance were performed using the two-tailed student's t-test for two groups, (control versus mutant, or media versus cell- or protein-treated limb, respectively). We considered $P < 0.05$ (indicated * in figures) as significant and $P < 0.01$ (**) as highly significant. All analysis was performed using Prism Graph Pad software.

RESULTS

CHAPTER 3

Overview: Adult Mesenchymal Stromal Cells Facilitate Axon Sorting and Myelination in Mice Deficient in Schwann Cell-Derived Laminin

Normal peripheral nerve development is dependent on a regulated process of axon and Schwann cell development.   Myelinated axons are sorted such that one Schwann cell envelops only one axon, and non-myelinated axons are completely encircled by non-myelinating Schwann cell cytoplasm. Congenital neuropathies in which these processes do not occur cause gross peripheral nerve dysfunction, for which there is no therapy. In this study, the sciatic nerves of mice in which both axon sorting and myelination fail to occur were treated with adult mesenchymal stromal cells derived from murine adipose tissue (mADSC). ADSC-treated mutant nerves showed improvement in hind-limb function as a result of improved axon sorting, myelination and diameter. ADSC-treated mutant nerve electrophysiology is consistent with these ultrastructural changes suggesting that these effects are functionally significant for the animals. Although the rare ADSC derivative can be found within the nerve parenchyma, the majority of ADSCs are localized to the perineurium of the mutant nerves.

These results suggest that mADSCs are providing stromal support for the mutant

nerves, and importantly, that this type of support is sufficient to facilitate

improvement in nerve function.

3.1 Stem cell treatment improves gross motor function

The laminin $\gamma 1^{-/-}$ mice are born in a normal litter size but exhibit poor survival

under normal conditions. These mice exhibit muscle wasting, increasingly poor

motor coordination that results in complete hind-limb paralysis by 21 days and

poor autonomic control that can result in death under conditions of high stress or

transport. With careful care, they can survive anesthetic and a surgical

procedure although many die in the process of stem cell or vehicle surgery(Z. L.

Chen and S. Strickland, 2003; W. M. Yu et al., 2005; W. M. Yu et al., 2007).

To examine the potential for adult stem cells to rescue function of laminin-

deficient sciatic nerves, one limb of the mutant mice was treated with 50,000

ADSCs and the contralateral limb was treated with stem cell growth media (J.

Fujimura et al., 2005). Within 14 days, gross motor improvements were visible in

the stem cell treated limbs. 3T3/L1 cells produce laminin and are a pre-adipocyte

non-stem cell line (T. Niimi et al., 1997) and were injected in place of ADSCs as a

cell-based control. This strategy allowed for direct comparison between limbs of

the same animal and alleviated concerns regarding variable penetrance of the

mutant phenotype. The 3T3/L1 cell treated mice did not exhibit gross improvements in motor function.

To measure changes in hindlimb function with ADSC or 3T3/L1 injection, electrophysiologic sciatic nerve measurements were pursued because it allows for quantitation along a number of parameters that describe nerve function (B. Johnsen and A. Fuglsang-Frederiksen, 2000; M. D. Weiss et al., 2001). The electrophysiologic equivalent of the gross motor observation is the MCST, which is a compound measurement of muscle-nerve function. Less current is needed to stimulate a muscle twitch in an intact neuromuscular unit. A similar strategy has been previously used to look at improvement in sciatic nerve function following hair follicle stem cell injection (Y. Amoh et al., 2005). Other behavioral measurements such as rotarod testing rely on improved limb function in all limbs for test performance and would not allow use of contralateral limbs as an internal control. For the purpose of comparison, MCST was also determined in sciatic nerves of mutant and control littermate mice that had not undergone prior surgery (**Table 1 and Figure 7A**). Untreated mutant animals required significantly more stimulus current to trigger downstream muscle twitch than did control littermates. Treatment of mutant nerves with ADSCs, but not with media or 3T3 cells resulted in significant improvement in motor function in comparison to surgical control

limbs, although MCST did not return to that of normal control littermates (**Table 1 and Figure 7B**). There was no significant difference in MCST between media-treated and untreated mutant nerves showing that the surgical procedure itself is not responsible for the improvement in MCST with ADSC treatment. These data demonstrate that enhancement of sciatic nerve function is possible after the onset of hind-limb paralysis. This finding is consistent with recent studies that indicating that mesenchymal stem cells can lead to improvements in peripheral nerve function in the context of injury models (H. C. Pan et al., 2007) as well as diabetic polyneuropathies models (T. Shibata et al., 2008).

Table 1. Sciatic nerve electrophysiology of control, mutant and cell- and laminin-treated mutant nerves.

Mouse Genotype	Nerve Conduction Latency (m/s)	Standard Error Margin	Number of Mice	Significance
Control	5.05	0.21	16	
Mutant	1.84	0.12	17	<0.0001
P0Lamg1$^{-/-}$ Mice + [Treatment] vs control limbs				
+ 3T3	2.69	0.15	7	0.21
+ ADSCs	3.91	0.33	9	0.0019
+ Laminin (soluble)	2.41	0.19	12	0.6272

Mouse Genotype	Compound Muscle Evoked Potential (mV)			
Control	18.4	1.4	15	
Mutant	2.40	0.59	14	<0.0001
P0Lamg1$^{-/-}$ Mice + [Treatment] vs control limb				
+ 3T3/L1	2.48	0.45	6	0.0247
+ ADSCs	6.27	1.02	11	0.0021
Laminin (soluble)	2.01	0.40	12	0.0467

Mouse Genotype	Minimum Current to Stimulate Twitch (mA)			
Control	150	30	12	
Mutat	680	50	11	0.0026
P0Lamg1$^{-/-}$ Mice + [Treatment]				
+ 3T3/L1	530	60	7	0.714
+ ADSCs	320	20	11	0.0001
+ Laminin (soluble)	580	40	12	0.947
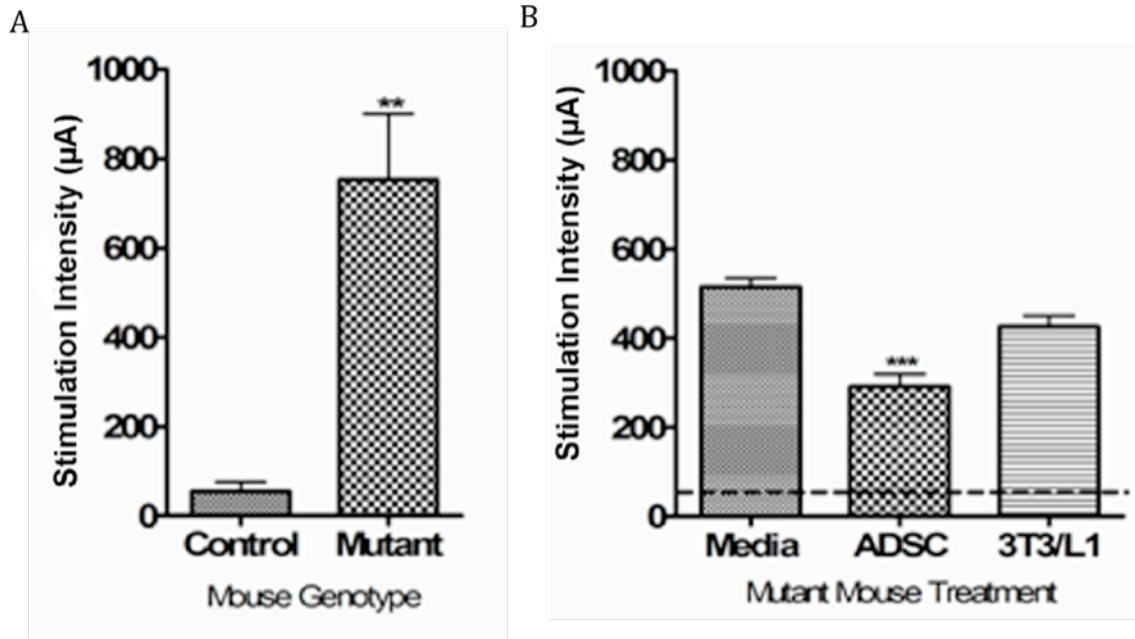
Figure 7. ADSC but not 3T3/L1 treatment of mutant sciatic nerves improves hind limb function by electrophysiology. (A) MCST was measured for mutant and littermate control (heterozygous for floxed Lamininγ1 allele and P0Cre transgene) sciatic nerves. **(B**) MCST was measured for mutant nerves that were treated either with DMEM or 5 x 10^5 F/F ADSCs or 3T3/L1 cells. Dashed line indicates the values for the control mice. * indicates p<0.05, ** indicates p<0.01, *** indicates P<0.001.

3.2 ADSCs are primarily localized to the perineurium

ADSCs injected around the sciatic nerves of mutant mice result in quantifiable improvement in hind limb motor function. This may have been a result of ADSC population of the mutant sciatic nerves and differentiation towards glia or neuronal cell types. Alternatively, ADSCs may have played a stromal support role without themselves replacing the endogenous and developmentally arrested cells and axons. To determine which was the case, ADSCs were labeled with DiI prior to injection and then examined the sciatic nerves were then examined by fluorescence microscopy to assess ADSC localization. Media treated controls did not result in DiI labeling, while 3T3-treated sciatic nerves contained trace amount of labeled cells. When nerves treated with ADSCs were analyzed at 7-days post transplant, Di-I labeled cells were visible on the perineurium. At the same time point at which MCST was measured and functional improvement was observed (21 days post-transplant), DiI-labeled ADSCs were extensively localized around the periphery of cell-treated sciatic nerves. Only rare DiI-labeled ADSCs were found within the nerve parenchyma. As anticipated, ADSCs did not form new neurons/axons, as DiI label never co-localized with neurofilament immunostaining (data not shown). These results suggest that ADSCs are providing stromal support for endogenous Schwann cells and axons rather than themselves myelinating axons. Mutant nerves treated with DiI-labeled

3T3/L1 cells did not contain surviving cells, consistent with their inability to mediate significant functional improvement in sciatic nerve function.

ADSC- treated nerves show morphological and physiological evidence of axon sorting and nascent myelin production, indicating that component(s) of the mutant nerves are being affected by ADSC injection. One possibility is that the endogenous Schwann cells are being pushed past their point of developmental arrest and are further sorting and myelinating axons. To determine whether this is the case, electron microscopy was used to examine sciatic nerves of mutant mice that had received treatment with ADSCs, 3T3/L1 cells or media.   There are sparse normally-myelinated axons in the mutant nerves. This myelin is derived from Schwann cells that either escaped recombination or are near an alternative source of laminin such as a capillary (Z.-L. Chen et al., 2003; Z. L. Chen and S. Strickland, 2003; W. M. Yu et al., 2005). All other axons are within unsorted axon bundles in which there are no Schwann cell cytoplasmic pojections separating axon membranes. The ultrastructure of media-treated limbs was identical to that untreated mutant sciatic nerves (**Figure 8A**). Although there were often Schwann cells near the axon bundles, they did not insert cytoplasmic extrusions between axon bundles nor encircle individual axons. Therefore there was no evidence of new myelination with media or surgery alone.

In the stem cell treated mutant nerves, there were bundles in which individual axons were sorted (**Figure 8B**). Multiple axons were fully encircled by cytoplasmic extrusions from adjacent glial-like cells fully encircling them, and some showed evidence of nascent myelination. Although this new myelin was not as thick as the myelin from a normal adult myelinated axon, it clearly had several layers. The glial cells that sort and myelinate axons also appeared to have associated basal lamina. These thinly myelinated axons with an associated glial basal lamina were never observed in untreated- (Z. L. Chen and S. Strickland, 2003; W. M. Yu et al., 2005), media-, or 3T3/L1 treated mutant nerves (**Figure 8C**).
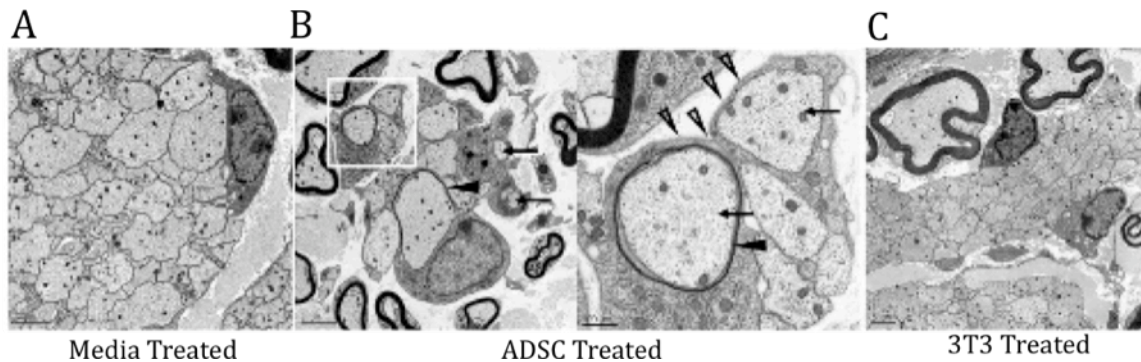
Figure 8. ADSC-treated nerves show morphologic evidence of nascent myelin production. Electron microscopy of media-treated sciatic nerves revealed ultrastructure that was unchanged from untreated mutant mice (W. M. Yu et al., 2005). The Schwann cell shown in panel **A** (arrowhead) is immature, without cytoplasmic extension into the adjacent axon bundle. (**B**) Twenty-one days after stem cell transplant, there was evidence of axons that were sorted and separated (arrows) from an unsorted bundle. There was also evidence of nascent myelin formation (arrowheads) and a basal lamina surrounding the glial cell sorting axons (open arrowheads). The area marked by the white box in the first panel is shown in higher magnification in the second panel. (**C**) EM of 3T3/L1 treated sciatic nerves failed to show any morphologic changes.

For nascent myelin formation to be functionally significant, it should result in electrophysiological changes consistent with improved myelination. Significant differences in axon sorting and myelination should be reflected in both nerve conduction latency (NCL), a measurement of the initiation of a motor response following nerve stimulation, and the maximum amplitude of the compound motor evoked potential (CMEP), which reflects the number and efficacy of axons capable of relaying current to the muscle. As a baseline, both parameters were measured in mutant and littermate control sciatic nerves.   Both parameters were significantly lower in mutant animals, consistent with the impaired axon sorting and myelination observed by electron microscopy (Z. L. Chen and S. Strickland, 2003; W. M. Yu et al., 2005) (**Table 1, Figures 9A and B**).

To determine any electrophysiological improvement in axon sorting and myelination, NCL and CMEP were determined for mutant mice after treatment with ADSCs, 3T3/L1 cells, and media (**Table 1, Figures 9C and D)**. NCL and CMEP were not significantly different between untreated and media-treated limbs, indicating that the surgery itself did not impact mutant sciatic nerve electrophysiology. Treatment of the mutant sciatic nerves with ADSCs significantly enhanced NCL and CMEP compared to treatment with media alone or with 3T3/L1 cells. These data show that the NCL in ADSC-treated nerves was equivalent to that of control nerves, suggesting drastically improved myelination for some axons (**Figure 8C and Table 1**). The CMEP of the mutant sciatic

46

nerves treated with stem cells versus media was also significantly improved,

showing a 3-fold increase from untreated mutant nerves (**Figure 9D and Table**

1). This result suggests that more axons are capable of transmitting current or

that less current is dissipated secondary to improved axon insulation, which is

consistent with the increased axon sorting and myelination seen by electron

microscopy.

.
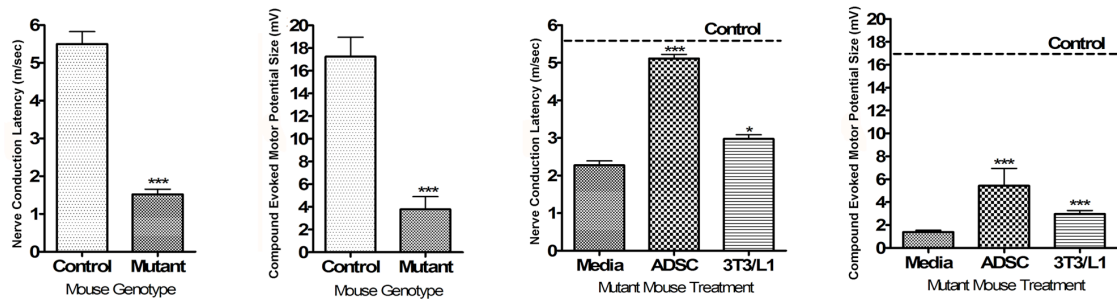
Figure 9. Electrophysiological profile of control and treated mutant mice.
NCL (**A**) and CMEP (**B**) of mutant and control mice were determined. (**C**) NCL
and (**D**) CMEP were measured for mutant nerves that were treated either with
DMEM or 5×10^5 F/F ADSCs or 3T3/L1 cells. For both NCL and CMEP, there
was significant improvement although not normalization in mutant sciatic nerves
following ADSC treatment. Treatment with 3T3/L1 cells induced a small but still
statistically significant improvement in both values. Dashed line indicates the
values for the control mice. * indicates p<0.05, ** indicates p<0.01, *** indicates
P<0.001.

3.3 ADSCs produce laminin in vitro following transplant

Schwann cell differentiation and axon myelination requires laminin. We further

investigated was whether ADSC expression of laminin was important for

functional, electrophysiologic or structural repair of the mutant nerves. ADSCs

grown in culture on poly-D Lysine coated coverslips were immunostained for

laminin expression using a polyclonal antibody that recognizes laminin subunits

α1, β1, and γ1. *In vitro*, laminin subunit expression was readily apparent in all

cells visualized. To examine ADSC-expression of laminin *in vivo*, DiI-labeled

ADSC-treated mutant nerves were collected and analyzed for laminin expression

by immunostaining. Although the majority of ADSCs do not co-localize with

laminin staining *in vivo*, some DiI-labeled cells can be found with an associated

laminin-containing basal lamina, suggesting that at least a subpopulation of

ADSCs do produce laminin in vivo as well.   Because laminin-expression by

ADSCs *in vitro* is widespread, it is also possible that the DiI labeled cells that are

not co-localized with a laminin-containing basal lamina secrete laminin, but have

not generated an organized basal lamina that can be detected by

immunofluoresence.

3.4 Soluble laminin alone is insufficient to mediate complete repair of mutant sciatic nerves

To determine if laminin alone was sufficient to mediate the functional, electrophysiologic, and morphologic changes observed in stem cell-treated nerves, soluble mouse laminin-1 was injected in place of ADSCs (**Figure 10 A-C**, **Table 1**). MCST, NCL and CMEP were not significantly improved from media treated nerves, showing that laminin-treated nerves did not show improvement in function or physiology.

In case there were subtle morphologic changes in the mutant sciatic nerves with soluble laminin injection, we also examined the ultrastructure of laminin-treated nerves (**Figure 10 D and E**). Nerve morphology was predominantly identical to that of media-treated nerves, although there were a few axon bundles in which cytoplasmic processes were beginning to sort and envelop individual axons. A single laminin injection was thus not as effective as a single ADSC-treatment since nascent myelination was never found in the laminin-treated nerves. Furthermore, functional or electrophysiologic measurements did not improve.
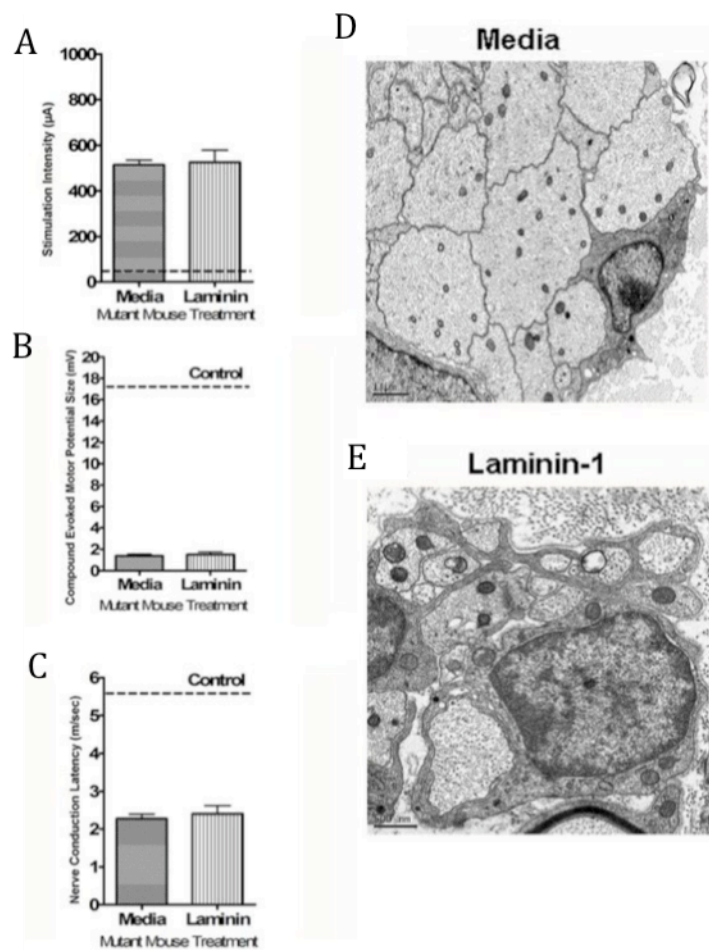
Figure 10. ADSCs produce laminin, however soluble laminin alone is insufficient to mediate complete rescue of mutant nerves. MCST (**A**), CMEP (**B**), and NCL (**C**) were measured for each of these treatment groups. Dashed line indicates the values for the control mice .* indicates p<0.05, ** indicates p<0.01, *** indicates P<0.001. Electron microscopy of media-treated nerves shows the axon bundles remain unsorted (**D**), while laminin-treated nerves show occasional initiation of sorting (**E**).

CHAPTER 4

Overview: **Maximum Entropy Network Analysis Reveals a Role for Tumor Necrosis Factor in Peripheral Nerve Development and Function**

Gene regulatory interactions that shape developmental processes can often be inferred from microarray analysis of gene expression, but most computational methods used require extensive data sets that can be difficult to generate. Here, we show that maximum entropy network analysis allows extraction of novel genetic interactions from limited microarray data sets. Maximum entropy networks indicated that the inflammatory cytokine TNF-alpha plays a pivotal role in Schwann cell-axon interactions, further suggesting that TNF mediates its effects by orchestrating cytoplasmic movement and axon guidance. *In vivo* and *in vitro* experiments confirmed these predictions, showing that Schwann cells in TNF-/- peripheral sensory bundles fail to envelop axons efficiently, and that recombinant TNF can partially correct these defects. These data demonstrate the power of maximum entropy network-based methods for analysis of microarray data, and indicate that TNF-alpha plays a direct role in Schwann cell-axon communication.

4.1 Entropy maximized network structure of DRG co-culture microarray is stable

Previous microarray studies of peripheral nerve development have used *in vivo* sciatic nerve tissue to cluster genes with similar transcriptional profiles(W. M. Yu et al., 2005; E. J. Ryu et al., 2008). The DRG co-culture system was used because the addition of ascorbic acid triggers the maturation of Schwann cell and neuronal interactions (R. Nagarajan et al., 2002), allowing finer temporal sampling than previously achieved: at 0, ½, 1, 6, 12, 24, 36, 48 hours post addition of ascorbic acid (**Figure 11A**). After choosing the 500 most variant transcriptional profiles (~2-3 fold changes from baseline), an individual interaction profile of each gene was constructed with all others in the network to determine an appropriate covariance cutoff score (**Figure 6**). The resulting pairwise interaction network was visualized when the cutoff score was defined as 2 or 3 standard deviations from a covariance score of 0 for individual interaction profiles. Under these conditions 148 and 70 genes, respectively, were included as nodes in the resulting map (**Figure 11B**). To determine if this network was representative of previously described scale-free genetic network structures, the number of links in each node was analyzed, and found it to be consistent (**Figure 11C**) (E. Ravasz et al., 2002; A. F. Svenningsen et al., 2003; A. Fernandez, 2007). The nodes with the greatest number of links were consistent if the covariance cutoff score was set at 2 or 3 standard deviations, indicating that the

network structure was stable (**Table 2**). The DRG co-culture network hubs

included netrin-1, Chemokine (C-X-C motif) ligand 2, EDAR-associated death

domain and TNF— all members of the NFkB transcriptional network (A. H. Tong

et al., 2004; M. J. Barallobre et al., 2005; A. Morlon et al., 2005; N. K. Phulwani et

al., 2008). These proteins encoded by these genes are involved in neurite

outgrowth, axon insulation and the activation of Schwann cells (M. P. Mattson,

2003; A. Paradisi et al., 2008a).
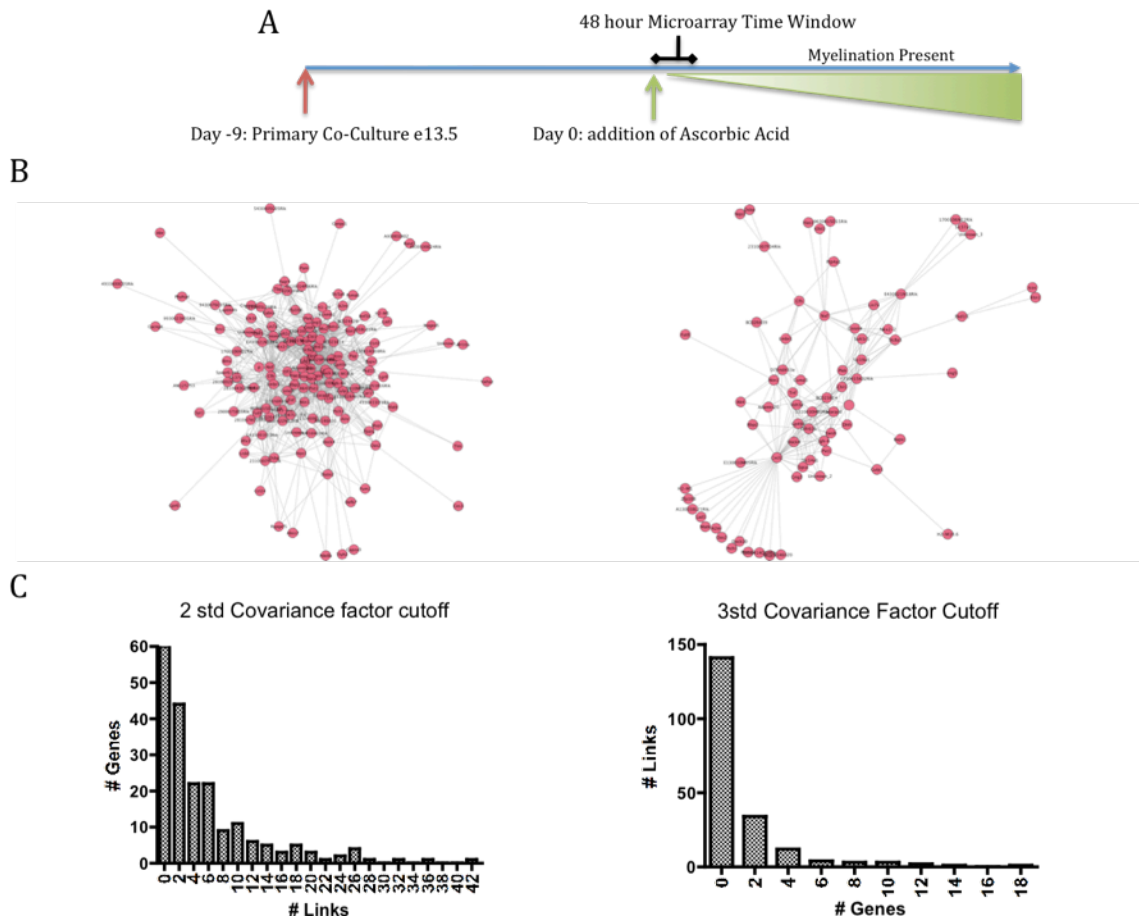
Figure 11: Entropy maximized network structure of DRG co-culture microarray. (A) Triplicate samples of wild type DRG co-cultures were obtained at 0, ½, 1, 6, 12, 24, 36, and 48 hour after the addition of ascorbic acid. (B) Visualization of the resulting entropy maximized network with 2 and 3 standard deviation covariance factor cutoffs, with 148 and 70 genes included, respectively. (C) For the 2 and 3 standard deviation cutoff, the number of links is plotted against the number of genes in the network as a histogram, defining influential genes as those with the most network interconnections.

Table 2: Highly linked gene nodes are similar in order and composition across 2 and 3 standard deviation covariance factor cutoffs, indicating that the network structure is stable.

# links	Gene Name	# links	Gene Name
2std Covariance Cutoff		**3std Covariance Cutoff**	
41	Glycoprotein 49 A	17	Glycoprotein 49 A
36	cDNA seq BC023814	13	cDNA seq BC023814
31	Cyclin M4	11	Tumor Necrosis Factor
27	Usher syndrome 3A homolog	11	Netrin 1
26	Chl1 CAM	10	Sulfotransferase family, cytosolic, 1C, member 1
25	Tumor Necrosis Factor	10	Cyclin M4
25	Solute Carrier Family 8, member 3	9	Chl1 CAM
25	Riken cDNA 1110030H02	8	Solute Carrier Family 8, member 3
24	Riken cDNA F730015K02	8	Riken cDNA 1110030H02
21	Sulfotransferase family, cytosolic, 1C, member 1	7	Chemokine (C-X-C motif) ligand 2
20	Netrin 1	6	EDAR-associated death domain
20	GULP, engulfment adaptor PTB domain 1	5	Riken cDNA F730015K02
19	Solute carrier family 19, member 3	5	Solute carrier family 19, member 3
17	Limb region 1	4	Dihydrofolate reductase
17	EDAR-associated death domain	4	GULP, engulfment adaptor PTB domain 1

4.2 TNF is a network hub in peripheral nerve development that links cellular processes

 TNF emerges as a highly linked node as the covariance cutoff stringency increases (**Table 2**). Previous studies have shown that TNF is involved in the activation of Schwann cells, long-term potentiation of sensory nerve fibers after injury and the development of neuropathic pain (W. M. Campana, 2007; S. Hao et al., 2007; S. J. Armstrong et al., 2008). The first degree neighbors of TNF were isolated in the model network and explored the literature for known interactions with TNF or TNF related signaling networks (**Figure 12**). Of the 11 genes in the local TNF network, two major groups of genes with related signaling components emerged on an axis of decreasing connectedness to other local TNF network genes. The group with a greater degree of network connectedness with TNF was related to NFkB, which has a well characterized role in the transcriptional regulation of peripheral nerve development. This group included netrin-1, which plays a role in axon guidance. The second group includes genes related to networks involved in cytoplasmic extension, enervation and Schwann cell function (K. Hiramoto et al., 2006; I. Hester et al., 2007; L. Jiang and S. T. Crews, 2007; Y. L. Liu et al., 2007; G. Upadhyay et al., 2008; Y. Zhang et al., 2008) (**Table 3**). TNF is tightly connected with the first group at the more fundamental level of transcriptional control related to NFkB, as compared to the

cellular effectors represented in the second group, suggesting that TNF is a

network node that intersects with these two groups.
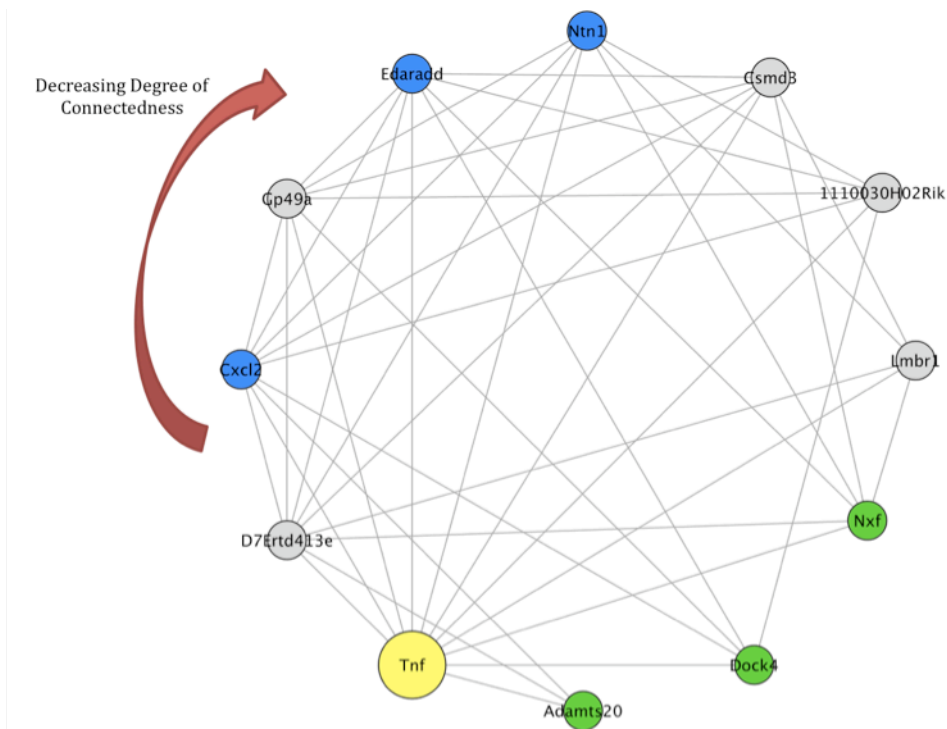
Figure 12: The first-degree neighbor network of TNF at a 3 standard deviation covariance factor cutoff includes two major groups of genes in decreasing degrees of connectedness, those that have NF-kappaB related functions (blue nodes) and those that have functions related to beta-catenin signaling and motor proteins (green nodes).

Table 3: Reported biological functions and relationships of genes included in the TNF first-neighbor network.

# Links within TNF network	Gene Name	Reported biological function/ relationships	Citations
9	DNA segment, Chr 7, ERATO Doi 413, expressed	N/A	N/A
9	Chemokine (C-X-C motif) ligand 2	NF-kappaB and TNF signalling in astrocytes	Phulwani *et al*.
8	Glycoprotein 49 A	Implicated in calcium mobilization, cytokine gene transcription	Lee KH *et al*
7	EDAR-associated death domain	TNF-receptor adaptor, activator of NF-kappaB pathway	Morlon A *et al*.
7	Netrin 1	Axonal guidance, under transcriptional regulation by NF-kappaB	Barallobre *et al.,* Paradisi *et al.*
7	Csmd3	Gene candidate for familial myoclonic epilepsy and autism	Floris C *et al., Shimizu* et al.
6	Riken cDNA 1110030H02	N/A	N/A
5	Limb region 1	Polydactyly and sonic hedge hog signalling	Hill RE *et al*.
5	bHLH-PAS type transcription factor NXF	mRNA dynamics with motor proteins, neuroprotection, *dysfusion* analog	Takano K *et al.,* Hester I *et al.,* Jiang L and Crews ST
5	Dock 4	Regulated by RhoG, promotes Rac-dependent cell migration, wnt/beta-catenin signalling	Hiromoto K *et al.,* Upadhyay G *et al*
3	Adamts20	Mediator of beta-catenin signalling in hair follicle pigmentation and innervation	Zhang Y *et al*.

4.3 TNF-/- mice experience sensory latency to thermally painful stimuli

In order to assess the role of TNF in peripheral nerve function, gross phenotypic

defects in TNF-/- sciatic nerves were analyzed. Previous studies have indicated

that anti-TNF neutralizing antibody reduces peripheral nerve sensory function in

pain models as well as in normal patients (M. Schafers et al., 2001; C. Sommer

et al., 2001; W. M. Campana, 2007; S. Hao et al., 2007; K. Takano et al., 2007),

potentially through ion channels in nociceptive neurons (C. Sommer et al., 1998).

Sensory function was assessed in response to thermal stimuli using the hot plate

test. Wild-type mice withdrew their paws significantly faster than TNF -/- mice

(P=0.0082), indicating that TNF-/- mice experience sensory latency (**Figure

13A**). In order to assess differences in motor function between the TNF-/- and

wild-type mice, a rotarod test was used. There were no significant differences in

motor performance (**Figure 13B**), indicating that interactions between

myelinating Schwann cells and axons are functional.

A

Hot Plate Sensory Test

B

Rotarod Motor Test
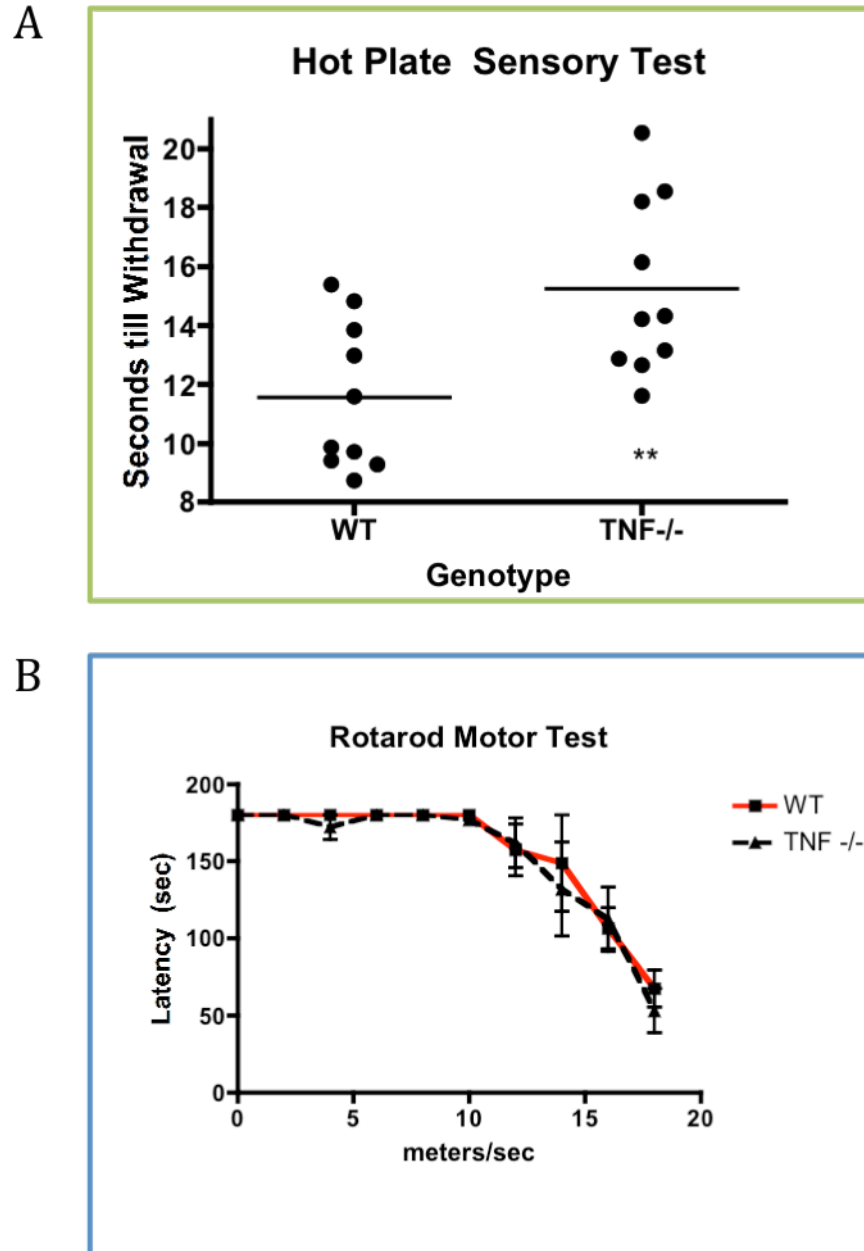
Figure 13: TNF -/- mice have sensory but not motor defect. (A) TNF-/- mice have significantly increased sensory latency as compared to wild type mice using the hot plate sensory test (P=0.0093) and (B) there is no significant difference between the motor function of wild type and TNF-/- mice.

4.4 TNF-/- mice have abnormal axon size variation in Remak sensory bundles

To order to explore the basis of the sensory latency in TNF -/- mice, cross sections of the Remak bundles were compared in sciatic nerve cross sections of 21 day old wildtype and TNF-/- mice. Remak sensory bundles convey pain information through the interaction of individual Schwann cells with multiple axons. As compared to wildtype mice, the Remak bundles of TNF-/- mice appeared to have greater axonal size variation and decreased circularity (**Figure 14A**). We analyzed the images using ImageJ software to quantitate these perceived differences, and found significantly greater variation in axonal size in TNF-/- Remak bundles (F-test, $P<0.00001$), but not in circularity (F-test, $P<.07534$) (**Figure 14B**). Closer examination of the Remak bundles revealed poor incorporation of axons in Schwann cell cytoplasm and incomplete envelopment (**Figure 15**). These results suggested that TNF is involved in the process of axonal envelopment by Schwann cell cytoplasm as well as modulation of axonal size, supporting previous molecular studies describing local interactions between Schwann cells and axons (J. C. Czeschik et al., 2008).
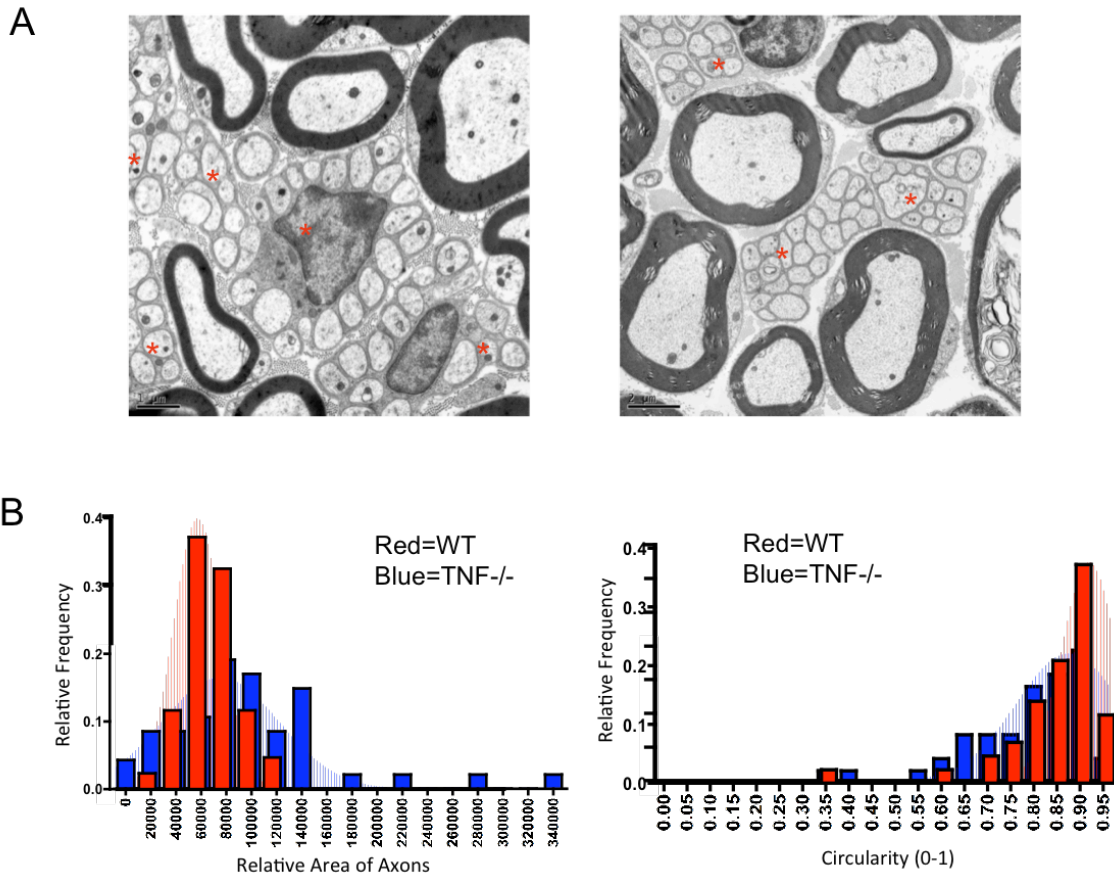
Figure 14: TNF-/- mice have significant variation in the area of axons within sciatic nerve Remak/Sensory bundles. (A) Electron micrographs of Remak bundles (*) suggest differences in the circularity and size variation of axons in wild type vs TNF-/- mice sciatic nerves. (B) The relative variation of area of axons in wild type vs. TNF-/- Remak sensory bundles is significant (P<0.0001), with more outliers in axonal size in TNF-/- sciatic nerves. The variation in Remak axon circularity did not meet significance (P=0.7534).
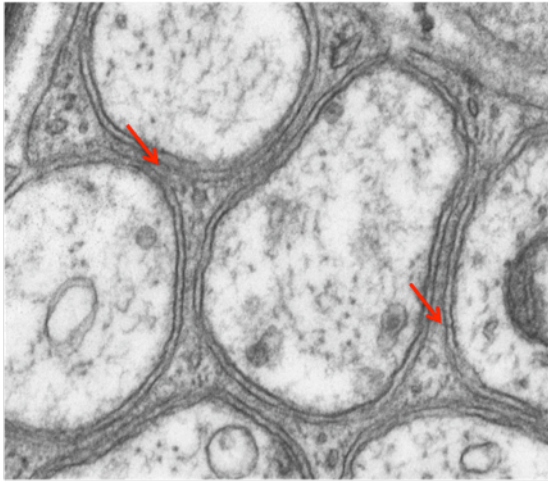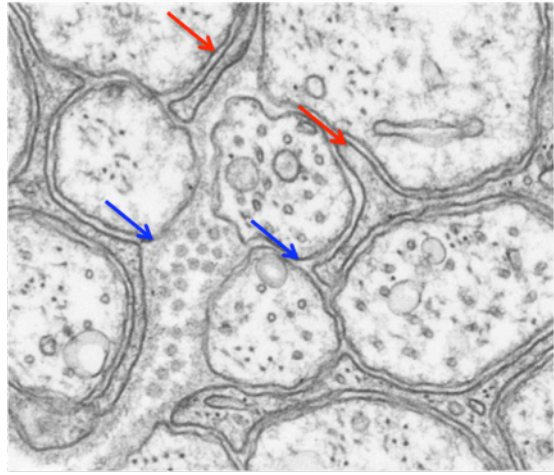
WT   TNF

Figure 15. Closer examination of Remak bundle schwann cell-axon relationships revealed greater spaces between TNF-/- schwann cells and axons (red arrows), as well as incomplete schwann cell cytoplasmic envelopment of axons (blue arrows) resulting in adjacent, uninsulated axons.

4.5 Non-myelinating Schwann cells in TNF-/- DRG co-cultures do not efficiently incorporate axons

In order to investigate the relationship between Schwann cells and axons, DRG co-cultures from TNF-/- and wild-type mice were generated for analysis by electron microscopy (**Figure 16A**). Both TNF-/- and WT mature DRG co-cultures contained myelinated axons and Schwann cells with multi-axon relationships. Schwann cells can myelinate one axon or envelop multiple non-myelinated axons. These latter Schwann cells are characterized by the envelopment of multiple, circular axons with short cytoplasmic extensions at the leading edge in wildtype co-cultures (**Figure 16B**). In TNF-/- co-cultures, multiple unmyelinated axons were juxtaposed with Schwann cells that have extensive cytoplasmic extensions rather than enveloped into the cytoplasm (**Figure 16C**). The axons also appeared to be irregularly shaped with wide size variation. To determine whether the differences in axon envelopment were significant, the number of axons juxtaposed with and enveloped in the cytoplasm of non-myelinating Schwann cells was assessed. Wildtype Schwann cells have significantly fewer axons juxtaposed with them as compared to TNF-/- Schwann cells (1.0 vs 4.3, P=0.0012) (**Figure 16D**). These same wildtype Schwann cells had significantly more axons enveloped in their cytoplasm than those in the TNF-/- co-culture (8.1 vs 2.0, P=0.009) (**Figure 16E**). These results suggest that there is a decrease in

functional interaction between non-myelinating Schwann cells and axons in the

absence of TNF.
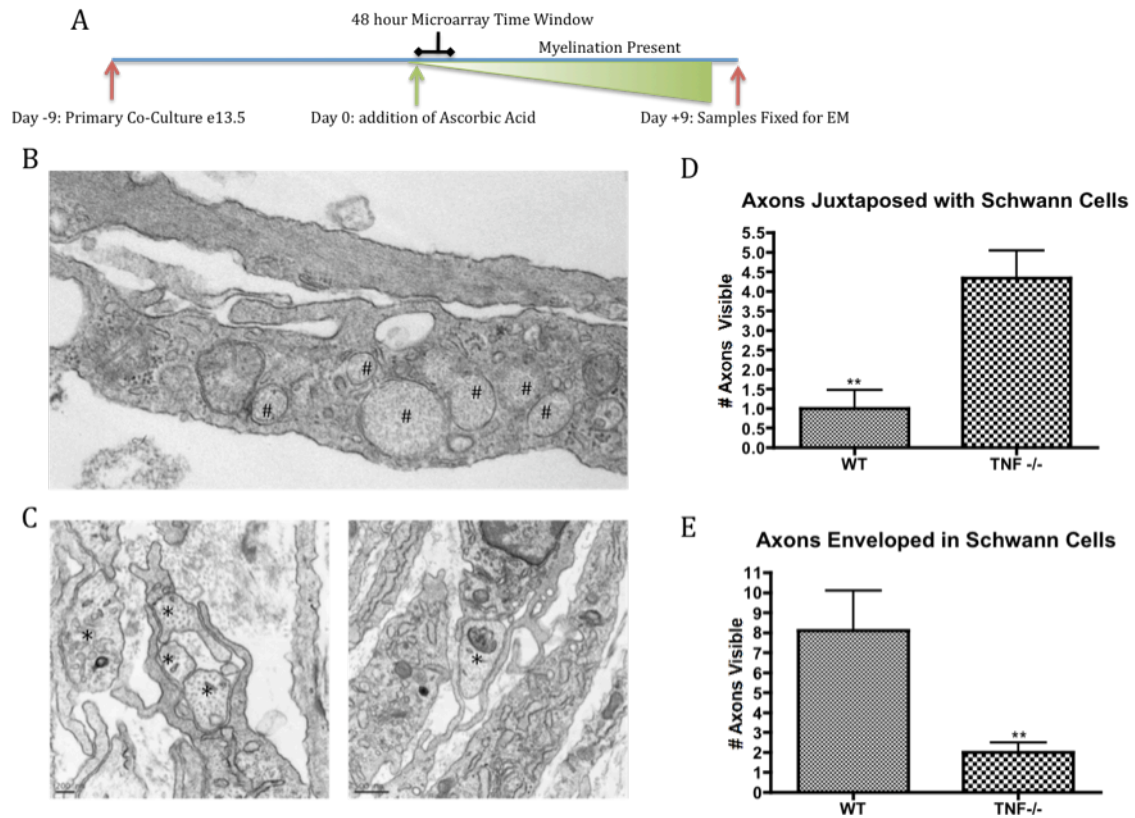
Figure 16: TNF-/- non-myelinating schwann cells do not efficiently envelop axons. (A) Timeline for fixation of co-culture samples in preparation for EM, allowing time for the maturation of myelinating schwann cell-axon interactions. (B) Wild type schwann cells envelop multiple axons into their cytoplasm (#), which have a uniformly round appearance. (C) TNF-/- schwann cells extend long cytoplasmic processes in search for axons while bypassing potential productive interactions (*). (D) The number of axons directly juxtaposed with schwann cells is significantly higher in TNF-/- co-cultures (P=0.0012) and (E) The number of axons enveloped by the same schwann cell (as quantified in D) cytoplasm is significantly higher in wild-type co-cultures (P=0.009).

4.6 The administration of anti-TNF antibody disrupts non-myelinating Schwann cell-axon interactions

Previous studies have shown that blocking TNF receptors mediates a decrease in sensory function in models of thermal, mechanical and neuropathic pain sensitization (C. Sommer et al., 1998; C. Sommer et al., 2001; G. V. Michailov et al., 2004). We speculated that the mechanism of decreased pain is due to disruptions in Schwann cell/multi-axon interactions. The effect of saturating quantities of TNF blocking antibody was explored for different durations (added at day -3, -1, 0; IgG antibody was added on day -3) in the wildtype co-culture system prior to the addition of ascorbic acid (time 0) according to the timeline shown in **Figure 17A**. The number of axons juxtaposed with Schwann cells was significantly higher when TNF-blocking antibody was added at day -3 as compared to control antibody (Day -3, 3.44 vs 0.44; P=0.0005)(**Figure 17B**). Conversely, the number of axons enveloped by Schwann cells was significantly lower (Day -3, 1.0 vs 9.67; P<0.0001)(**Figure 17C**). Electron micrographs of non-myelinating Schwann cell-axon interactions in the presence of IgG or anti-TNF antibody are shown in **Figure 17D**, depicting the increase in juxtaposed axons and decrease in enveloped axons when the TNF pathway is disrupted.

In order to understand the spatial localization of TNF in relation to Schwann cells and neurons, immunofluorescence was performed with IgG and TNF blocking

antibody (day-3) treatment. In the presence of a control antibody, Schwann cells

and neurons overlap while TNF is found in localized plumes next to the cells. In

contrast, Schwann cells and neurons do not overlap in the presence of TNF-

blocking antibody, and TNF localized around cells (**Figure 18A**). The expression

of netrin-1 and TNF receptor 1 is correlated to NFkB transcription (M. Empl et al.,

2001; G. M. Kim et al., 2001). The localization of netrin-1 in relation to TNF and

TNF receptor 1 was examined to determine the validity of a network predicted

relation. In the presence of a control antibody, netrin-1 was present in localized

aggregates while the TNF receptor 1 was relatively diffuse and this relationship

was inverted in the presence of TNF blocking antibody (**Figure 18B**). Together

these findings indicate that TNF signaling and netrin-1 act in concert to mediate

Schwann cell-axonal interactions along with TNF receptor 1. TNF signaling

pathway is a necessary component of physiologic Schwann cell-axonal

interactions and is specifically disrupted in the presence of TNF blocking
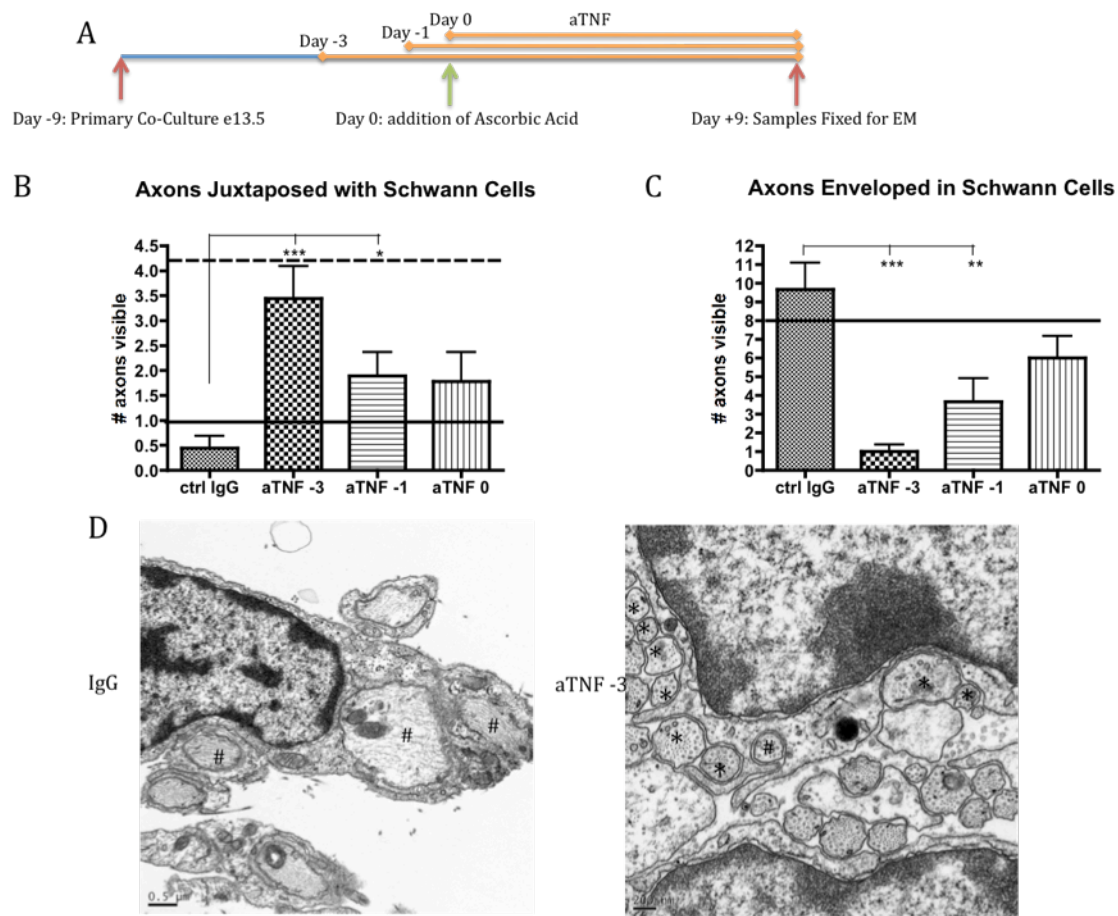
antibody.

Figure 17. TNF-blocking antibody administration (aTNF) in WT DRG co-cultures results in decreased schwann-cell axon envelopment. (A) aTNF and Control IgG added at Day -3, along with aTNF at Day -1 and Day 0 until samples fixed for EM at Day +9. (B) The number of axons juxtaposed with Schwann cells is significantly increased when aTNF is administrated at Day -3 as compared to control antibody (3.44 vs 0.44, P=0.005). (C) The number of axons enveloped by Schwann cells is significantly decreased when aTNF is administrated at Day -3 as compared to control antibody (1.00 vs 9.67, P<0.0001). (D) Electron micrograph of control antibody and TNF blocking antibody treatment at Day -3 showing an increase in axons juxtaposed to schwann cells with TNF blocking antibody treatment (*)
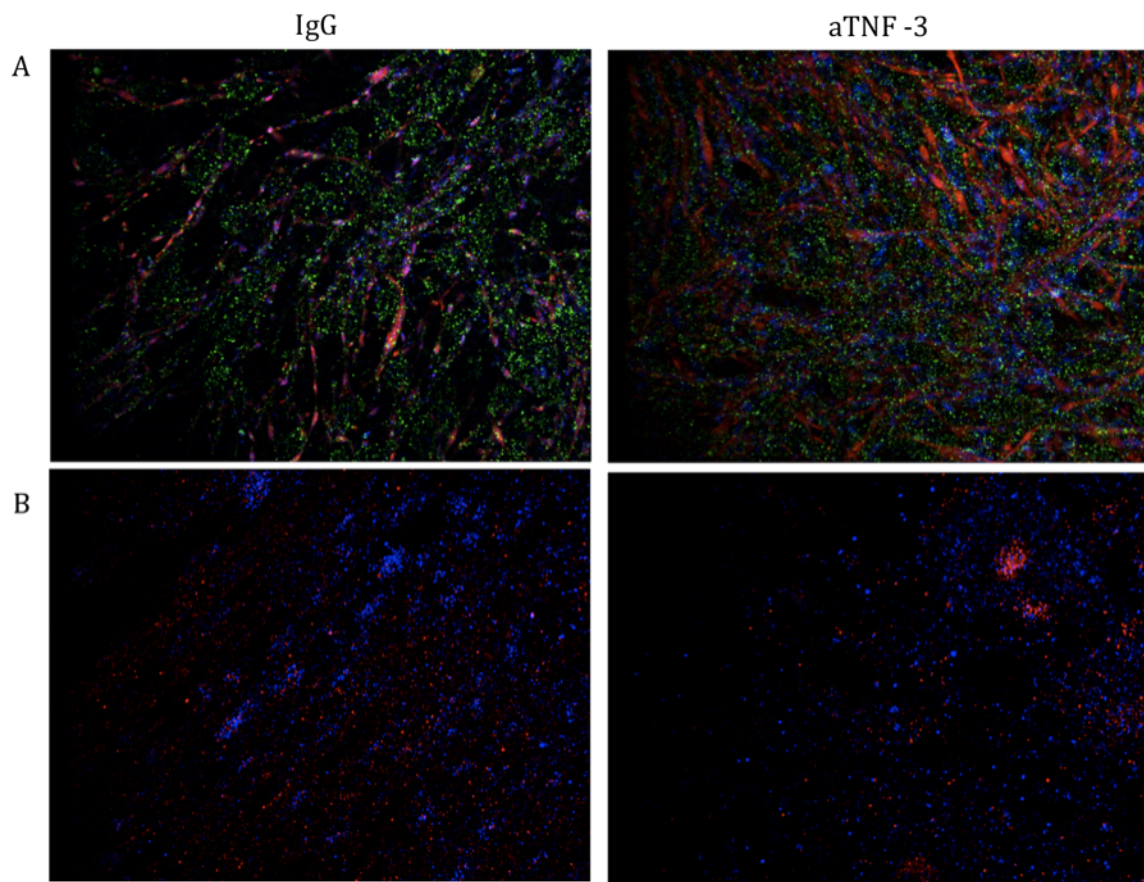
Figure 18. Localization of TNF, Netrin 1 and TNFR1 is modulated in the presence of aTNF. (A) Immunofluorescence of co-cultures with control IgG and TNF blocking antibody of neurons (red), schwann cells (blue) and TNF (green). Schwann cells and neurons co-localize with control antibody administration, as compared to separation evident with TNF blocking antibody, and TNF expression is localized vs diffuse. (B) Netrin-1 (blue) is clustered and TNFR1 is diffuse in the presence of control antibody while this relationship is switched in the presence of TNF blocking antibody.

4.7 rmTNF partially restores impaired Schwann cell/multi-axon interactions in TNF-/- co-cultures

To order to determine if impaired Schwann cell/multi-axon interactions in TNF-/- co-cultures could be restored, rmTNF was added in 10-fold dilution (5ng/ml, 0.5ng/ml, 0.05ng/ml) to co-cultures at day -3 until fixation at day +9 (**Figure 19A**). The addition of 5ng/ml of rmTNF resulted in significantly fewer axons juxtaposed with Schwann cells as compared to 0.5ng/ml and 0.05ng/ml (p=0.025 and p=0.044, respectively) (**Figure 19B**). Conversely, the addition of 5ng/ml of rmTNF resulted in significantly more axons enveloped in Schwann cells as compared to 0.5ng/ml (p=0.028) (**Figure 19C**). Electron micrographs of Schwann cell-axonal interactions with 0.5ng/ml depict Schwann cell cytoplasmic extensions enveloping an axon (dashed black line, **Figure 19D** inset) adjacent to a fully incorporated axon. With 5ng/ml of rmTNF the Schwann cell cytoplasm continued to encircle multiple axons (solid black arrows, **Figure 19D** inset) rather than fully incorporating them. Increasing concentrations of rmTNF partially disrupted TNFR1 clusters (red) and resulted in partial netrin-1 (blue) clustering, indicating that rmTNF administration does not fully restore TNF-/- co-cultures to match wildtype markers (**Figure 20**). These data indicate that initial Schwann cell-axon interactions of recognition and envelopment are mediated by TNF, and that further incorporation of axons into the Schwann cell cytoplasm is mediated by other factors.
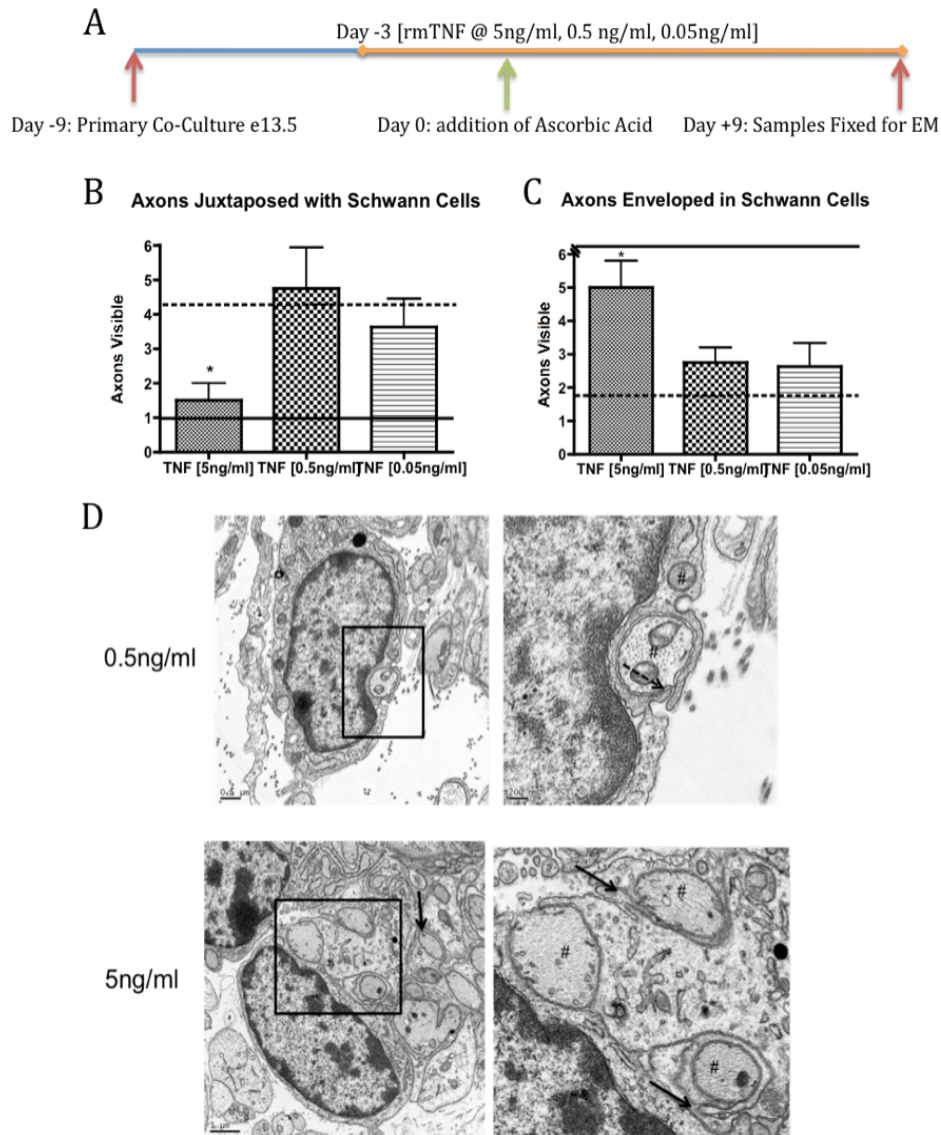
Figure 19. rmTNF partially restores Schwann cell-axonal interactions in TNF-/- co-cultures (A) rmTNF administered at Day -3 at 5ng/ml, 0.5ng/ml and 0.05ng/ml. (B) The administration of 5ng/ml of rmTNF results in significantly fewer juxtaposed axons to Schwann cells as compared to a 10-fold lower dose (1.50 vs 4.75, p=0.025). (C) The administration of 5ng/ml of rmTNF results in significantly more axons enveloped in schwann cell cytoplasm as compared to a 10-fold lower dose (5.00 vs 2.75, p=0.028). (D) Electron micrograph of Schwann cell-axonal interactions with 0.5ng/ml rmTNF and 5ng/ml depicting Schwann cell cytoplasmic extensions enveloping multiple axons (dashed black line) and encircling multiple axons (solid black arrows) in the inset.
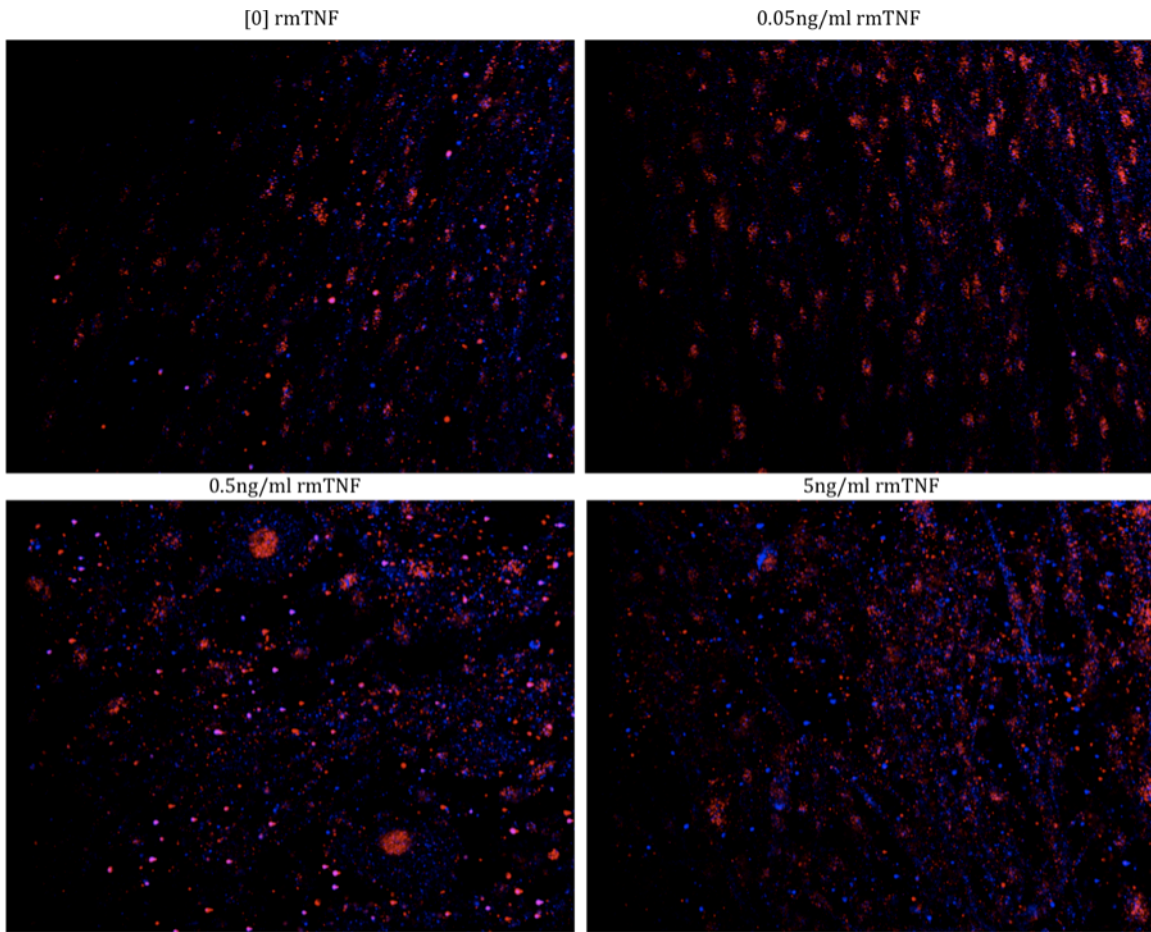
Figure 20. Increasing concentrations of rmTNF partially disrupt TNFR1 clusters (red) and result in partial netrin-1 (blue) clustering.

CHAPTER 5

DISCUSSION

5.1 Crossing the Therapeutic Threshold into Functionality

In many instances of injury or hereditary disease, the PNS is able to repair itself

or compensate to achieve function. However, adequate peripheral nerve repair

does not occur in congenital or even some acquired neuropathies. The data

presented here show evidence that mesenchymal stem cell therapy has the

potential to improve function in congenital or long-lived laminin-associated

peripheral neuropathies such as CMD1A.

There has been a recent surge of interest in the use of mesenchymal stem cells

as biological therapy. This interest is related to the risk of unwanted teratoma

formation and thus severe limitations when using less differentiated cell types

such as embryonic stem cells. The immune-privileged status and

immunomodulatory effect of mesenchymal stem cells, and their role as a stromal

support cell for a variety of tissue types.

Our results show that mesenchymal ADSCs have the potential to induce

functional and structural repair of developmentally dysregulated peripheral

nerves. This is most likely an indirect effect of ADSCs on endogenous Schwann

cells and axons, although there may be some small contribution from ADSC differentiation into myelin-producing cells. The occasional appearance of sorted axon bundles without nascent myelin formation following laminin injection shows that the endogenous laminin-deficient Schwann cells retain the potential to overcome their developmental arrest and begin axon sorting. ADSCs may also mediate improvement in mutant nerve physiology by providing a continuous laminin source within the laminin-deficient nerve parenchyma, or may produce neurotrophins that could stimulate the increased axon diameter.

One possible explanation for the lack of improvement in electrophysiology and nascent myelination despite improved axon sorting following soluble laminin-injection could be that laminin-1 (α1, β1, γ1) was used, while the predominant laminin found in adult sciatic nerves is laminin-2 (α2, β1, γ1). However, soluble laminin-1 has been used *in vitro* to completely rescue axon myelination defects in laminin-2 deficient dorsal root ganglia co-cultures (unpublished results) (S. C. Previtali et al., 2003; A. Paradisi et al., 2008b), and two of the three subunits are identical. This seems like an unlikely reason for the lack of rescue with laminin injections. Alternative explanations for the failure of a single injection of laminin to improve function and electrophysiology and only partially alter ultrastructure of mutant nerves include the absence of continuous laminin secretion or neutrotrphin secretion by ADSCs.

The focus of future studies based on this work will necessarily encompass further clarification of the role of laminin and the ECM in mesechymal stem cell function

and identification of the exact factors that the ADSCs supply the mutant nerves and trigger changes in nerve morphology and physiology.

5.2 Locating the Therapeutic Threshold of Vulnerability

To our knowledge, this is the first study where gene candidate predictions made employing maximum entropy networks have been experimentally confirmed to reveal novel functional information, suggesting that this process is a useful approach to prioritize studies of complex interactions using pre-existing or new microarray data. Maximum entropy analysis of microarray data differs from clustering because it moves beyond covariance to describe the interrelated structure of complex systems such as gene networks. Because previous microarray datasets used to explore the utility of maximum entropy analysis in genetic networks have either been periodic, heavily sampled or have included transcriptional profiles that vary far greater than ~2-3 fold (R. Pittier et al., 2005), we did not expect functionally thematic neighborhood network maps from our data. We were encouraged by the presence of genes with known or tangentially related function to nervous system development, function or attendant cellular processes. By exploring a wild-type process in an *in vitro* DRG co-culture model system, we showed that TNF is a predicted component of normal maturation of Schwann cell-neuronal interactions via maximum entropy network analysis. The

availability of transgenic mice and molecular tools made TNF an ideal choice for exploring the relationship between a cytokine in the context of endogenous peripheral nerve function. Further analysis of the first-degree TNF network implicated intersecting signaling processes that involve components of the NFkB transcriptional pathways as well as downstream cytoplasmic motor function. These components have been previously implicated in Schwann cell and axonal function, providing sufficient information to construct a hypothesis in concert with published literature.

TNF-/- mice showed increased latency to thermal stimuli and normal motor function, suggesting that there would be abnormalities in the Remak bundles of sciatic nerves. The spatial constraints of an organized tissue provide structural boundaries that can minimize the effects of dysfunctions that would be more apparent in cell culture. We returned to the disrupted DRG tissue that comprises the co-culture system in order to exploit this potential. Through histologic and DRG co-culture analysis of TNF-/- mice by electron microscopy, we demonstrated that Schwann cell/multi-axonal interactions were disrupted. These data suggest that TNF mediates communication between Schwann cells and axons in concert with associated signaling networks during peripheral nerve development, including netrin-1 signaling. This is underscored by partial restoration of Schwann cell-axon interactions in TNF-/- co-cultures in the presence of rmTNF. The pursuit of TNF was also motivated by clinical studies of

anti-TNF antibody treatment that implicate TNF's role in the nervous system as secondary to immune reactions. Further experimental studies have shown that TNF is capable of acting as a primary effector of nervous system function. We found that administration of anti-TNF antibody in the *in vitro* DRG co-culture system recapitulated the effects of the TNF-/- mice, suggesting that it is possible to induce impaired sensory function by modulating access to TNF signaling networks between non-myelinating Schwann cells and axons. This, however, does not preclude the possibility that TNF may act on the peripheral nervous system as a cytokine. These findings indicate that patients undergoing systemic administration of anti-TNF antibody should be carefully monitored for the management of neuropathies that emerge during the course of treatment. Although we suggest signaling networks for further exploration, the precise molecular interactions that mediate this complex phenotype remain unclear. The availability of TNF neighborhood networks in conjunction with known signaling transduction pathways will facilitate the elucidation of the molecular mechanisms.

The maximum entropy network we describe to explore the role of TNF can be broadly applied to the richly available microarray data of complex processes and can provide an entrée to understanding relevant molecular relationships. The network we describe in this study has been limited to the 500 most variant genes during the 48 hours following the triggering of a maturation process between two dominantly represented cell types. As the time boundaries and experimental

conditions change, variant network maps will emerge. If these variant networks

are mapped in relation to each other, it will be possible to better understand the

common molecular network features that underlie complex processes across

tissues. In the meantime, screening of predicted gene candidates should be

informed by the availability of resources, cost of exploration and clinical

relevance. This process is depicted in **Figure 21**. We suggest that in order to

exercise the utility of preexisting microarray data, entropy should be maximized

as part of an orderly process.
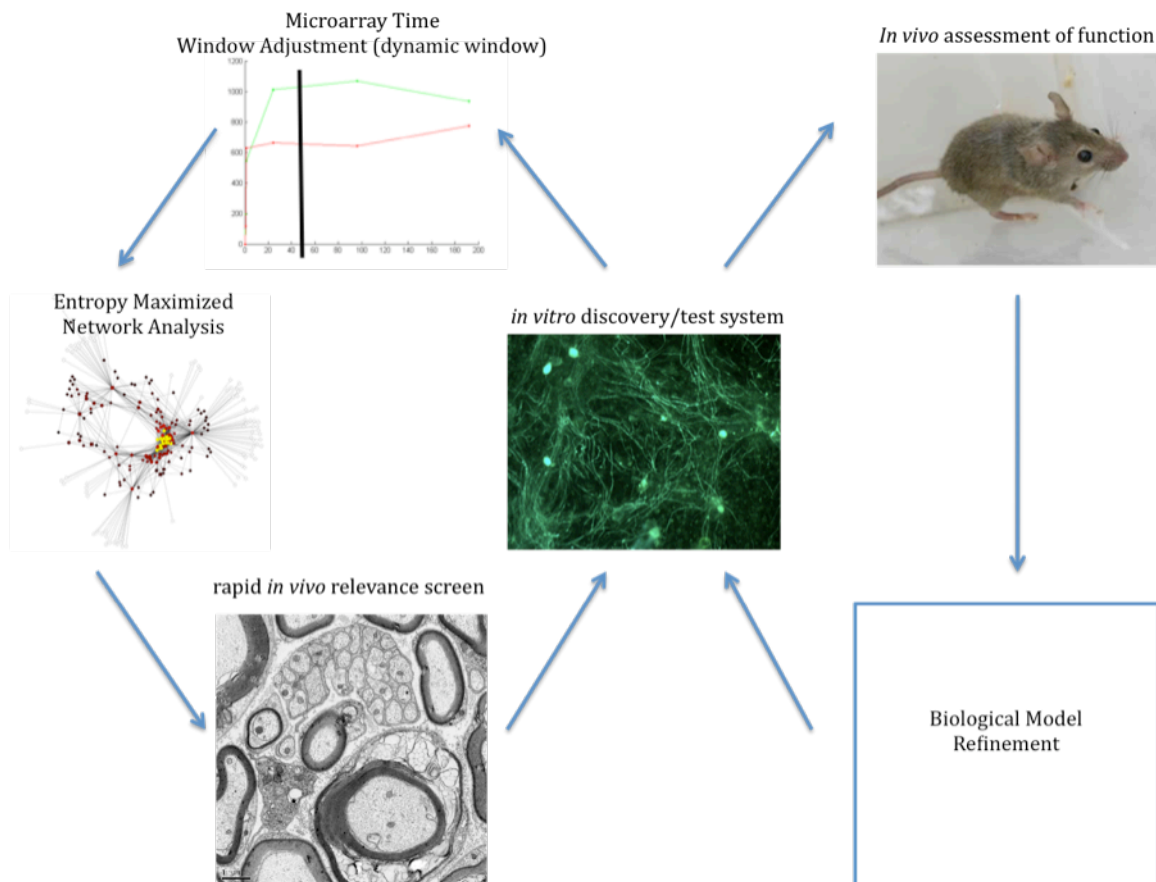
Figure 21. Process for gene candidate assessment and model refinement via network analysis. Microarray analysis of an *in vitro* experimental system is used to generate an entropy maximized network structure that isolates highly linked gene candidates. Depending on the system, a rapid *in vivo* screen for histological and functional relevance will indicate if further experimental follow-up is warranted within this schema. If so, further rounds of *in vitro* experimentation, followed by potential reframing of the microarray time window or conditions can lead to biological model refinement that reflects the dynamic nature of complex systems.

CHAPTER 6

FURTHER STUDY

There are three potential steps that could result in the merging of these parallel

studies, allowing the insight of each to bear upon the other. In this section,

evidence for further study and speculative reasoning will be used to chart a path

forward. First, information from this study will be integrated with evidence from

the central and peripheral nervous system to describe a homeostatic function of

TNF in physiologic context. Secondly, experiments to determine the molecular

mechanisms of the role of TNF in peripheral experiment will be explored. Thirdly,

in the course of describing evidence that points to ADSCs as potential source of

TNF, we will describe a possible experimental system for future work.

TNF in Neural Systems

In 1985, the Cerami lab reported that a molecular that played a key role in the

development of sepsis, Cachectin, was the same as Tumor Necrosis Factor.

Tumor Necrosis Factor was given its name for the remarkable *in vitro* ability of

this molecule to specifically destroy developing tumors. The excitement about

this function led to Phase II clinical trials for safety in humans that were halted

due to unexplained toxicity in patients. The reason for this toxicity became

immediately clear when two streams of experimental work merged showing that

Tumor Necrosis Factor/Cachectin (TNF), were in fact the same molecular. In a remarkable stream of studies, the Cerami group showed that the same ability to kill tumors was responsible for lethal sepsis and wasting in animals and humans (B. A. Beutler et al., 1985; J. M. Dayer et al., 1985; K. J. Tracey et al., 1987; A. Cerami and B. Beutler, 1988; B. Beutler and A. Cerami, 1989; Y. Fong et al., 1989; T. R. Lezon et al., 2006).

As studies of the role of TNF in wasting progressed, it became clear that TNF had broad systemic effects on metabolism and protein redistribution. Further studies showed that TNF has direct effects on the synthesis of endocrine hormones. It is now known to be a powerful modulator of Neuroendocrine function ranging from adrenal stimulation to glucocorticoid production to melatonin synthesis (J. M. Dayer et al., 1985; K. J. Tracey et al., 1988; R. Braczkowski et al., 1995; I. J. Elenkov et al., 2000; G. di Comite et al., 2006; P. A. Fernandes et al., 2006).

The connection between the Neuroendocrine system and TNF was further strengthened when a group reported that stimulation of the vagus nerve results in the inhibition of TNF production at nerve terminals, now termed the "inflammatory reflex" (I. J. Elenkov et al., 1992). Extensive work done by the McEwen laboratory has demonstrated that the environmental inputs and outputs of the Neuroendocrine system contribute to the "allostatic load" on the physiological state, which can result in organ level dysfunction in the context of chronic stress (K. J. Tracey, 2002; B. McEwen and E. N. Lasley, 2003).

At the molecular scale, experimental work using anti-TNF antibody has demonstrated that neuropathic pain can be diminished. Obversely, the injection of TNF alpha into the endoneurium induces neuropathic pain behaviors. Since neuropathic pain response requires central nervous system integration, current evidence suggests that local administration or ablation of TNF triggers an integrative response (B. S. McEwen, 1998; T. A. Ignatowski et al., 2005; P. Dubovy et al., 2006; S. Sharma et al., 2007).

Finally, The role of TNF in blunting or exacerbating neurological effects has been most recently shown in a model of ischemic brain injury where TNFR1 directly facilitate the action of erythropoietin and VEGF to achieve a protective effect (R. Wagner and R. R. Myers, 1996). These studies coupled with the work presented here suggest that TNF may play an integrative role at the axis of the nervous, immune and endocrine systems. So where do these broadly suggestive but largely disparate studies leave us in light of the work presented here?

The work presented in this study makes it possible to speculate that one mechanism for the role of TNF in the nervous system may be the selective modulation of physical associations between Schwann cells and axons. There is precedent for this suggested physical mechanism in the role of astroglial pseudopodia retraction and extension in the hypothalamic-pituitary axis in response to oxytocin levels, which is where TNF mediates some of its effects on melatonin and glucocorticoid synthesis. The evidence presented above indicates that in the presence of TNF, associations between glial cells and axons increase

while the addition of anti-TNF antibody results in looser association. A

modulatory activity rather than a binary of association/disassociation is within the

dynamic operating range evident in the quantitation of envelopment in TNF-/- and

WT sciatic nerves and co-cultures (see Figure 15 and 17). Furthermore, the

addition of rTNF appears to result in "tighter" association rather than cytoplasmic

fusion and envelopment. This proposed mechanism is speculative, but is

motivated by understanding how the intersection of TNF in various nervous

system contexts can have pleitropic effects on multiple systems such as the

endocrine system. A plausible mechanism must allow for a local mechanism to

manifest itself in a heterogeneous manner given its context. For instance, this

fits with a scenario of neuropathic pain where the addition of rTNF intensifies pain

behaviors while anti-TNF antibody diminishes it. In order to explore this

possibility further, the molecular mechanisms of this interaction must be

elucidated.

Molecular Action of a "TNF Zipper"

In order to understand the molecular mechanisms of TNF and TNFR1 in

mediating the envelopment and release of axons by Schwann cells, further

studies must establish whether TNF is membrane bound or soluble. TNF can be

cleaved by TACE, a metalloprotease to release it from its membrane bound

state. This could be better understood by an experiment where a dominant

negative of the TNFR1 trimer or TNF is expressed in the cytoplasm of neurons or Schwann cells. Previous studies indicate that it is most likely that Schwann cells express TNFR1 as well as TNF, and should be the first hypothesis tested due to the relative ease of transfection over neurons. The studies presented strongly indicate that the TNFR1 is membrane bound, although the localization of TNF is less clear. Though would be difficult to visualize soluble TNF in the manner presented in Figure 18, it is possible that TNF is membrane bound in proximity to TNFR1 until it is cleaved by TACE or other metalloproteases. This would allow the membrane bound TNFR1 to associate into functional trimers with the appropriate concentration of TNF ligand. This is testable in an experimental system by modulating levels of TNF, TACE or TNFR1 to achieve productive signaling through known pathways such as MAPK outputs.

The patch and dispersion of TNFR1 and netrin-1 are likely a result of concentration dependence on levels of rTNF through a mechanism called homesis. From toxicology, this term describes a dynamic concentration curve where too little or too much ligand or receptor can block productive interactions through associations that are too tight or too loose. A situation of tight association may result in multiple layers of Schwann cell encircling axons without fusion as seen with high concentrations of rTNF in Figure 19 and 20. It is possible that TNF and TNFR1 associate to form a "TNF zipper" that results in the association of Schwann cell membranes and axons while precluding envelopment and fusion. The productive modulation of this relationship provides

a mechanism for the modulation of glial cell-axon relationships suggested above.

This possibility requires rigorous experimental work to develop this speculative

hypothesis.

ADSCs and TNF

The concentration of TNF and TNFR1 in an *in vitro or in vivo* system are likely to

substantially effect the outcome of any experiment depending on the

concentration, duration and location of administration – potentially at extremely

sensitive ranges. Further studies will require a more context appropriate and

localized delivery vehicle to modulate levels of TNF. As presented in the first

study, ADSCs can serve as physiologically appropriate vehicles to deliver

functionally critical components. Recent reports indicate that angiotensin

regulates differentiation of ADSCs through the modulation of TNF. ADSCs

express high lvels of TNF, which are down regulated as ADSCs commit to

adipose cell lineages (**Figure 22**) (R. A. Memon et al., 1993). It would be useful

to determine if the expression of TNF by ADSCs in the TNF$^{-/-}$ DRG co-culture

model would result in rescue of axonal-Schwann cell disruption with or without

fusion defects. The variance of angiotensin levels in the co-culture would result

in the modulation of TNF delivery by ADSCs. If this approach is successful, stem

cells could serve as a natural tool for delivering contextually appropriate amounts

of a target molecule without knowing the quantity beforehand. This would be a
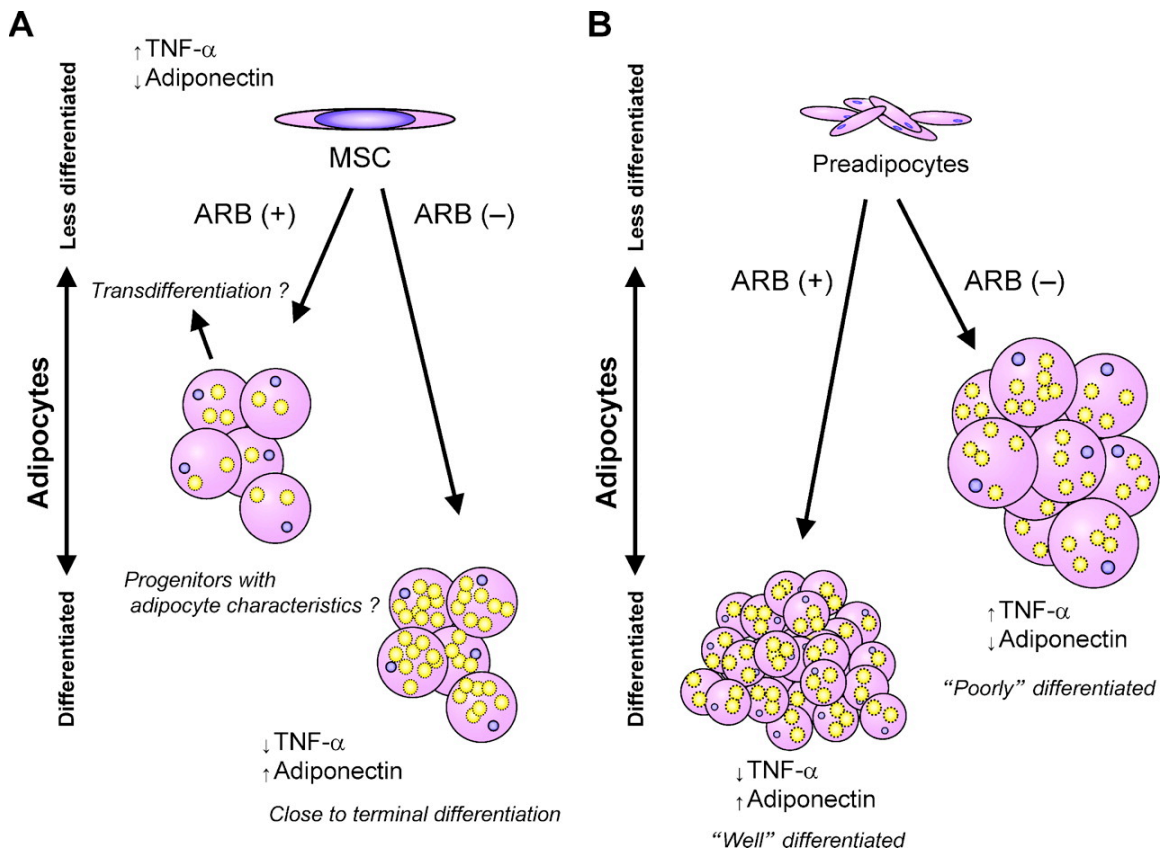
Figure 22. Two different mechanisms of adipocyte differentiation. (A) In differentiated adipocytes TNF-, is decreased and beneficial cytokines such as adiponectin are increased whereas the opposite is observed in MSCs. (B) Preadipocytes treated with an ARB differentiate into small adipocytes and secrete decreased inflammatory cytokines, such as TNF- and increased beneficial cytokines, such as adiponectin, and are regarded as well-differentiated adipocytes.(M. Mogi et al., 2006)

powerful way to study the effect of broadly influential but locally sensitive molecules such as TNF. This system allows for a dynamic quantity of target molecule delivered by tuning the stem cell differentiating factor, which has potentially fewer local effects in the system in question.

Conclusions and Final Thoughts

Further questions remain about the utility of maximum entropy network analysis in uncovering functional interactions. The relationship between the TNF neighborhood network and the rest of the network map is unclear. The molecular interactions suggested by the neighborhood network still require further study, especially in the case of netrin-1. While this type of analysis may not select for a particular type of biological function, it is likely this procedure selects for those sets of molecules that have broadly interconnected relationships given the data and context presented. The nature of these interactions is likely to be most evident in a dynamic ongoing process like peripheral nerve development. If this system was at rest, it is more likely that cyclically functional genes would be identified that may be of lower magnitude than those listed in Appendix A. This analysis will likely result in the loss of crucial subnetworks and network relationships, but the relationships presented provide a strong hypothesis generating basis for further experimentation.

APPENDIX A

List of Genes from Maximum Entropy Analysis by # of links at the three standard deviation cutoff (from original list of 200 most variable genes). Genes that had 0 links are not included below.

Gp49a	17	Mus musculus glycoprotein 49 A (Gp49a), mRNA.
BC023814	13	Mus musculus cDNA sequence BC023814 (BC023814), mRNA.
Tnf	11	Mus musculus tumor necrosis factor (Tnf), mRNA.
Ntn1	11	Mus musculus netrin 1 (Ntn1), mRNA.
Sult1c1	10	Mus musculus sulfotransferase family, cytosolic, 1C, member 1 (Sult1c1), mRNA.
Cnnm4	10	Mus musculus cyclin M4 (Cnnm4), mRNA.
Chl1	9	Mus musculus cell adhesion molecule with homology to L1CAM (Chl1), mRNA.
Slc8a3	8	Mus musculus solute carrier family 8 (sodium/calcium exchanger), member 3 (Slc8a3), mRNA.
1110030H02Rik	8	Mus musculus RIKEN cDNA 1110030H02 gene (1110030H02Rik), mRNA.
Cxcl2	7	Mus musculus chemokine (C-X-C motif) ligand 2 (Cxcl2), mRNA.
	6	
Edaradd	6	Mus musculus EDAR (ectodysplasin-A receptor)-associated death domain (Edaradd), mRNA.
F730015K02Rik	5	Mus musculus RIKEN cDNA F730015K02 gene (F730015K02Rik), mRNA.
Slc19a3	5	Mus musculus solute carrier family 19 (sodium/hydrogen exchanger), member 3 (Slc19a3), mRNA.
Unknown_2	4	Mus musculus DNA cross-link repair 1A, PSO2 homolog (S. cerevisiae) (Dclre1a), mRNA.
Ush3a	4	Mus musculus Usher syndrome 3A homolog (human) (Ush3a), mRNA.
Dhfr	4	Mus musculus dihydrofolate reductase (Dhfr), mRNA.
Gulp1	4	Mus musculus GULP, engulfment adaptor PTB domain containing 1 (Gulp1), mRNA.
Lmbr1	4	Mus musculus limb region 1 (Lmbr1), mRNA.
Csmd3	4	
Cfh	4	Mus musculus complement component factor h (Cfh), mRNA.
Slc14a1	3	Mus musculus solute carrier family 14 (urea transprorter), member 1 (Slc14a1), mRNA.
Plek	3	Mus musculus pleckstrin (Plek), mRNA.
Sgca	3	Mus musculus sarcoglycan, alpha (dystrophin-associated glycoprotein) (Sgca), mRNA.
Adamts20	3	Mus musculus a disintegrin-like and metalloprotease (reprolysin type) with thrombospondin type 1 motif, 20 (Adamts20), mRNA.
Nxf	3	Mus musculus bHLH-PAS type transcription factor NXF (Nxf), mRNA.
Ptp4a1	2	Mus musculus protein tyrosine phosphatase 4a1 (Ptp4a1),

		mRNA.
Rbp2	2	Mus musculus retinol binding protein 2, cellular (Rbp2), mRNA.
Pxt1	2	
Ewsh	2	
Ak4	2	Mus musculus adenylate kinase 4 (Ak4), mRNA.
Olfr616	2	Mus musculus olfactory receptor 616 (Olfr616), mRNA.
Lin7a	2	Mus musculus lin 7 homolog a (C. elegans) (Lin7a), mRNA.
Unknown_3	1	Mus musculus aspartate-beta-hydroxylase (Asph), mRNA.
Ing5	1	Mus musculus inhibitor of growth family, member 5 (Ing5), mRNA.
Lad1	1	Mus musculus ladinin (Lad1), mRNA.
1700106N22Rik	1	Mus musculus RIKEN cDNA 1700106N22 gene (1700106N22Rik), mRNA.
9630015D15Rik	1	Mus musculus RIKEN cDNA 9630015D15 gene (9630015D15Rik), mRNA.
A2m	1	Mus musculus alpha-2-macroglobulin (A2m), mRNA.
Fut8	1	Mus musculus fucosyltransferase 8 (Fut8), mRNA.
Rbm12	1	Mus musculus RNA binding motif protein 12 (Rbm12), transcript variant 1, mRNA.
A130038L21Rik	1	Mus musculus RIKEN cDNA A130038L21 gene (A130038L21Rik), mRNA.
E130010M05Rik	1	Mus musculus RIKEN cDNA E130010M05 gene (E130010M05Rik), mRNA.
5330414O08Rik	1	Mus musculus RIKEN cDNA 5330414O08 gene (5330414O08Rik), mRNA.
Klhl1	1	Mus musculus kelch-like 1 (Drosophila) (Klhl1), mRNA.
Hao3	1	Mus musculus hydroxyacid oxidase (glycolate oxidase) 3 (Hao3), mRNA.
Bapx1	1	Mus musculus bagpipe homeobox gene 1 homolog (Drosophila) (Bapx1), mRNA.
Icos	1	Mus musculus inducible T-cell co-stimulator (Icos), mRNA.
Slc37a1	1	Mus musculus solute carrier family 37 (glycerol-3-phosphate transporter), member 1 (Slc37a1), mRNA.
Ptch1	1	Mus musculus patched homolog 1 (Ptch1), mRNA.
Ktn1	1	Mus musculus kinectin 1 (Ktn1), mRNA.
H2-M1	1	Mus musculus histocompatibility 2, M region locus 1 (H2-M1), mRNA.
Zfp108	1	Mus musculus zinc finger protein 108 (Zfp108), mRNA.
Nqo1	1	Mus musculus NAD(P)H dehydrogenase, quinone 1 (Nqo1), mRNA.
Osbp	1	
Matk	1	Mus musculus megakaryocyte-associated tyrosine kinase (Matk), mRNA.
AW146020	1	Mus musculus expressed sequence AW146020 (AW146020), mRNA.
Dock4	1	
BC026439	1	Mus musculus cDNA sequence BC026439 (BC026439), mRNA.

REFERENCES:

Akutsu T, Miyano S, Kuhara S (2000) Algorithms for identifying Boolean networks and related biological networks based on matrix multiplication and fingerprint function. J Comput Biol 7:331-343.

Alm E, Arkin AP (2003) Biological networks. Curr Opin Struct Biol 13:193-202.

Almaas E, Oltvai ZN, Barabasi AL (2005) The activity reaction core and plasticity of metabolic networks. PLoS Comput Biol 1:e68.

Amoh Y, Li L, Campillo R, Kawahara K, Katsuoka K, Penman S, Hoffman RM (2005) Implanted hair follicle stem cells form Schwann cells that support repair of severed peripheral nerves. Proc Natl Acad Sci U S A 102:17734-17738.

Andorfer B, Kieseier BC, Mathey E, Armati P, Pollard J, Oka N, Hartung HP (2001) Expression and distribution of transcription factor NF-kappaB and inhibitor IkappaB in the inflamed peripheral nervous system. J Neuroimmunol 116:226-232.

Armstrong SJ, Wiberg M, Terenghi G, Kingham PJ (2008) Laminin activates NF-kappaB in Schwann cells to enhance neurite outgrowth. Neurosci Lett 439:42-46.

Arroyo EJ, Bermingham JR, Jr., Rosenfeld MG, Scherer SS (1998) Promyelinating Schwann cells express Tst-1/SCIP/Oct-6. J Neurosci 18:7891-7902.

Azuaje F (2002) A cluster validity framework for genome expression data. Bioinformatics 18:319-320.

Barabasi AL, Oltvai ZN (2004) Network biology: understanding the cell's functional organization. Nat Rev Genet 5:101-113.

Barallobre MJ, Pascual M, Del Rio JA, Soriano E (2005) The Netrin family of guidance factors: emphasis on Netrin-1 signalling. Brain Res Brain Res Rev 49:22-47.

Berghoff M, Samsam M, Muller M, Kobsar I, Toyka KV, Kiefer R, Maurer M, Martini R (2005) Neuroprotective effect of the immune system in a mouse model of severe dysmyelinating hereditary neuropathy: enhanced axonal degeneration following disruption of the RAG-1 gene. Mol Cell Neurosci 28:118-127.

Bergsteinsdottir K, Kingston A, Mirsky R, Jessen KR (1991) Rat Schwann cells produce interleukin-1. J Neuroimmunol 34:15-23.

Beutler B, Cerami A (1989) The biology of cachectin/TNF--a primary mediator of the host response. Annu Rev Immunol 7:625-655.

Beutler BA, Milsark IW, Cerami A (1985) Cachectin/tumor necrosis factor: production, distribution, and metabolic fate in vivo. J Immunol 135:3972-3977.

Bolshakova N, Azuaje F (2006) Estimating the number of clusters in DNA microarray data. Methods Inf Med 45:153-157.

Bonetti B, Valdo P, Stegagno C, Tanel R, Zanusso GL, Ramarli D, Fiorini E, Turazzi S, Carner M, Moretto G (2000) Tumor necrosis factor alpha and human Schwann cells: signalling and phenotype modulation without cell death. J Neuropathol Exp Neurol 59:74-84.

Bourde O, Kiefer R, Toyka KV, Hartung HP (1996) Quantification of interleukin-6 mRNA in wallerian degeneration by competitive reverse transcription polymerase chain reaction. J Neuroimmunol 69:135-140.

Braczkowski R, Zubelewicz B, Romanowski W, Lissoni P, Barni S (1995) Modulation of tumor necrosis factor-alpha (TNF-alpha) toxicity by the pineal hormone melatonin (MLT) in metastatic solid tumor patients. Ann N Y Acad Sci 768:334-336.

Campana WM (2007) Schwann cells: activated peripheral glia and their role in neuropathic pain. Brain Behav Immun 21:522-527.

Cerami A, Beutler B (1988) The role of cachectin/TNF in endotoxic shock and cachexia. Immunol Today 9:28-31.

Chen Z-L, Indyk JA, Strickland S (2003) Exogenous soluble laminin-1 disrupts the endogenous laminin layer and promotes neuronal cell death in the

mouse hippocampus: Evidence for a dynamic extracellular matrix. submitted.

Chen ZL, Strickland S (2003) Laminin gamma1 is critical for Schwann cell differentiation, axon myelination, and regeneration in the peripheral nerve. J Cell Biol 163:889-899.

Chen ZL, Haegeli V, Yu H, Strickland S (2008) Cortical deficiency of laminin gamma1 impairs the AKT/GSK-3beta signaling pathway and leads to defects in neurite outgrowth and neuronal migration. Dev Biol.

Cheng C, Qin Y, Shao X, Wang H, Gao Y, Cheng M, Shen A (2007) Induction of TNF-alpha by LPS in Schwann cell is regulated by MAPK activation signals. Cell Mol Neurobiol 27:909-921.

Choi YS, Cha SM, Lee YY, Kwon SW, Park CJ, Kim M (2006) Adipogenic differentiation of adipose tissue derived adult stem cells in nude mouse. Biochem Biophys Res Commun.

Czeschik JC, Hagenacker T, Schafers M, Busselberg D (2008) TNF-alpha differentially modulates ion channels of nociceptive neurons. Neurosci Lett 434:293-298.

D'Haeseleer P (2005) How does gene expression clustering work? Nat Biotechnol 23:1499-1501.

D'Haeseleer P, Liang S, Somogyi R (2000) Genetic network inference: from co-expression clustering to reverse engineering. Bioinformatics 16:707-726.

Dayer JM, Beutler B, Cerami A (1985) Cachectin/tumor necrosis factor stimulates collagenase and prostaglandin E2 production by human synovial cells and dermal fibroblasts. J Exp Med 162:2163-2168.

di Comite G, Marinosci A, Di Matteo P, Manfredi A, Rovere-Querini P, Baldissera E, Aiello P, Corti A, Sabbadini MG (2006) Neuroendocrine modulation induced by selective blockade of TNF-alpha in rheumatoid arthritis. Ann N Y Acad Sci 1069:428-437.

Dubovy P, Jancalek R, Klusakova I, Svizenska I, Pejchalova K (2006) Intra- and extraneuronal changes of immunofluorescence staining for TNF-alpha

and TNFR1 in the dorsal root ganglia of rat peripheral neuropathic pain models. Cell Mol Neurobiol 26:1205-1217.

Eccleston PA, Mirsky R, Jessen KR, Sommer I, Schachner M (1987) Postnatal development of rat peripheral nerves: an immunohistochemical study of membrane lipids common to non-myelin forming Schwann cells, myelin forming Schwann cells and oligodendrocytes. Brain Res 432:249-256.

Elenkov IJ, Chrousos GP, Wilder RL (2000) Neuroendocrine regulation of IL-12 and TNF-alpha/IL-10 balance. Clinical implications. Ann N Y Acad Sci 917:94-105.

Elenkov IJ, Kovacs K, Duda E, Stark E, Vizi ES (1992) Presynaptic inhibitory effect of TNF-alpha on the release of noradrenaline in isolated median eminence. J Neuroimmunol 41:117-120.

Empl M, Renaud S, Erne B, Fuhr P, Straube A, Schaeren-Wiemers N, Steck AJ (2001) TNF-alpha expression in painful and nonpainful neuropathies. Neurology 56:1371-1377.

Featherstone DE, Broadie K (2002) Wrestling with pleiotropy: genomic and topological analysis of the yeast gene expression network. Bioessays 24:267-274.

Feltri ML, Wrabetz L (2005) Laminins and their receptors in Schwann cells and hereditary neuropathies. J Peripher Nerv Syst 10:128-143.

Feltri ML, D'Antonio M, Previtali S, Fasolini M, Messing A, Wrabetz L (1999) P0-Cre transgenic mice for inactivation of adhesion molecules in Schwann cells. Ann N Y Acad Sci 883:116-123.

Fernandes PA, Cecon E, Markus RP, Ferreira ZS (2006) Effect of TNF-alpha on the melatonin synthetic pathway in the rat pineal gland: basis for a 'feedback' of the immune response on circadian timing. J Pineal Res 41:344-350.

Fernandez A (2007) Molecular basis for evolving modularity in the yeast protein interaction network. PLoS Comput Biol 3:e226.

Fong Y, Moldawer LL, Marano M, Wei H, Barber A, Manogue K, Tracey KJ, Kuo G, Fischman DA, Cerami A, et al. (1989) Cachectin/TNF or IL-1 alpha induces cachexia with redistribution of body proteins. Am J Physiol 256:R659-665.

Friedman N (2004) Inferring cellular networks using probabilistic graphical models. Science 303:799-805.

Friedman N, Linial M, Nachman I, Pe'er D (2000) Using Bayesian networks to analyze expression data. J Comput Biol 7:601-620.

Fujimura J, Ogawa R, Mizuno H, Fukunaga Y, Suzuki H (2005) Neural differentiation of adipose-derived stem cells isolated from GFP transgenic mice. Biochem Biophys Res Commun 333:116-121.

Gee SH, Blacher RW, Douville PJ, Provost PR, Yurchenco PD, Carbonetto S (1993) Laminin-binding protein 120 from brain is closely related to the dystrophin-associated glycoprotein, dystroglycan, and binds with high affinity to the major heparin binding domain of laminin. J Biol Chem 268:14972-14980.

Hao S, Mata M, Glorioso JC, Fink DJ (2007) Gene transfer to interfere with TNFalpha signaling in neuropathic pain. Gene Ther 14:1010-1016.

Helbling-Leclerc A, Zhang X, Topaloglu H, Cruaud C, Tesson F, Weissenbach J, Tome FM, Schwartz K, Fardeau M, Tryggvason K, et al. (1995) Mutations in the laminin alpha 2-chain gene (LAMA2) cause merosin-deficient congenital muscular dystrophy. Nat Genet 11:216-218.

Hester I, McKee S, Pelletier P, Thompson C, Storbeck C, Mears A, Schulz JB, Hakim AA, Sabourin LA (2007) Transient expression of Nxf, a bHLH-PAS transactivator induced by neuronal preconditioning, confers neuroprotection in cultured cells. Brain Res 1135:1-11.

Hiramoto K, Negishi M, Katoh H (2006) Dock4 is regulated by RhoG and promotes Rac-dependent cell migration. Exp Cell Res 312:4205-4216.

Holter NS, Maritan A, Cieplak M, Fedoroff NV, Banavar JR (2001) Dynamic modeling of gene expression data. Proc Natl Acad Sci U S A 98:1693-1698.

Holter NS, Mitra M, Maritan A, Cieplak M, Banavar JR, Fedoroff NV (2000) Fundamental patterns underlying gene expression profiles: simplicity from complexity. Proc Natl Acad Sci U S A 97:8409-8414.

Hughes RA (2002) Peripheral neuropathy. BMJ 324:466-469.

Ideker T, Thorsson V, Ranish JA, Christmas R, Buhler J, Eng JK, Bumgarner R, Goodlett DR, Aebersold R, Hood L (2001) Integrated genomic and proteomic analyses of a systematically perturbed metabolic network. Science 292:929-934.

Ignatowski TA, Sud R, Reynolds JL, Knight PR, Spengler RN (2005) The dissipation of neuropathic pain paradoxically involves the presence of tumor necrosis factor-alpha (TNF). Neuropharmacology 48:448-460.

Jessen KR, Mirsky R (1997) Embryonic Schwann cell development: the biology of Schwann cell precursors and early Schwann cells. J Anat 191 (Pt 4):501-505.

Jessen KR, Mirsky R (2002) Signals that determine Schwann cell identity. J Anat 200:367-376.

Jessen KR, Mirsky R (2005) The origin and development of glial cells in peripheral nerves. Nat Rev Neurosci 6:671-682.

Jiang L, Crews ST (2007) Transcriptional specificity of Drosophila dysfusion and the control of tracheal fusion cell gene expression. J Biol Chem 282:28659-28668.

Johnsen B, Fuglsang-Frederiksen A (2000) Electrodiagnosis of polyneuropathy. Neurophysiologie clinique = Clinical neurophysiology 30:339-351.

Khanin R, Wit E (2006) How scale-free are biological networks. J Comput Biol 13:810-818.

Kim GM, Xu J, Song SK, Yan P, Ku G, Xu XM, Hsu CY (2001) Tumor necrosis factor receptor deletion reduces nuclear factor-kappaB activation, cellular inhibitor of apoptosis protein 2 expression, and functional recovery after traumatic spinal cord injury. J Neurosci 21:6617-6625.

Kuang W, Xu H, Vachon PH, Liu L, Loechel F, Wewer UM, Engvall E (1998) Merosin-deficient congenital muscular dystrophy. Partial genetic correction in two mouse models. J Clin Invest 102:844-852.

Lee DS, Park J, Kay KA, Christakis NA, Oltvai ZN, Barabasi AL (2008) The implications of human metabolic network topology for disease comorbidity. Proc Natl Acad Sci U S A 105:9880-9885.

Lee G, Kim H, Elkabetz Y, Al Shamy G, Panagiotakos G, Barberi T, Tabar V, Studer L (2007) Isolation and directed differentiation of neural crest stem cells derived from human embryonic stem cells. Nat Biotechnol 25:1468-1475.

Lezon TR, Banavar JR, Cieplak M, Maritan A, Fedoroff NV (2006) Using the principle of entropy maximization to infer genetic interaction networks from gene expression patterns. Proc Natl Acad Sci U S A 103:19033-19038.

Li S, Wu L, Zhang Z (2006) Constructing biological networks through combined literature mining and microarray analysis: a LMMA approach. Bioinformatics 22:2143-2150.

Liang S, Fuhrman S, Somogyi R (1998) Reveal, a general reverse engineering algorithm for inference of genetic network architectures. Pac Symp Biocomput:18-29.

Liao JC, Boscolo R, Yang YL, Tran LM, Sabatti C, Roychowdhury VP (2003) Network component analysis: reconstruction of regulatory signals in biological systems. Proc Natl Acad Sci U S A 100:15522-15527.

Liebermeister W (2002) Linear modes of gene expression determined by independent component analysis. Bioinformatics 18:51-60.

Liu YL, Zhou LJ, Hu NW, Xu JT, Wu CY, Zhang T, Li YY, Liu XG (2007) Tumor necrosis factor-alpha induces long-term potentiation of C-fiber evoked field potentials in spinal dorsal horn in rats with nerve injury: the role of NF-kappa B, JNK and p38 MAPK. Neuropharmacology 52:708-715.

Martyn CN, Hughes RA (1997) Epidemiology of peripheral neuropathy. J Neurol Neurosurg Psychiatry 62:310-318.

Matsumura K, Yamada H, Saito F, Sunada Y, Shimizu T (1997) Peripheral nerve involvement in merosin-deficient congenital muscular dystrophy and dy mouse. Neuromuscul Disord 7:7-12.

Mattson MP (2003) Insulating axons via NF-kappaB. Nat Neurosci 6:105-106.

McEwen B, Lasley EN (2003) Allostatic load: when protection gives way to damage. Adv Mind Body Med 19:28-33.

McEwen BS (1998) Stress, adaptation, and disease. Allostasis and allostatic load. Ann N Y Acad Sci 840:33-44.

Memon RA, Grunfeld C, Moser AH, Feingold KR (1993) Tumor necrosis factor mediates the effects of endotoxin on cholesterol and triglyceride metabolism in mice. Endocrinology 132:2246-2253.

Meyer zu Horste G, Hu W, Hartung HP, Lehmann HC, Kieseier BC (2008) The immunocompetence of Schwann cells. Muscle Nerve 37:3-13.

Michailov GV, Sereda MW, Brinkmann BG, Fischer TM, Haug B, Birchmeier C, Role L, Lai C, Schwab MH, Nave KA (2004) Axonal neuregulin-1 regulates myelin sheath thickness. Science 304:700-703.

Mirsky R, Jessen KR (1996) Schwann cell development, differentiation and myelination. Curr Opin Neurobiol 6:89-96.

Mirsky R, Stewart HJ, Tabernero A, Bradke F, Brennan A, Dong Z, Jessen KR (1996) Development and differentiation of Schwann cells. Rev Neurol (Paris) 152:308-313.

Mirsky R, Jessen KR, Brennan A, Parkinson D, Dong Z, Meier C, Parmantier E, Lawson D (2002) Schwann cells as regulators of nerve development. J Physiol Paris 96:17-24.

Mogi M, Iwai M, Horiuchi M (2006) Emerging concept of adipogenesis regulation by the renin-angiotensin system. Hypertension 48:1020-1022.

Morlon A, Munnich A, Smahi A (2005) TAB2, TRAF6 and TAK1 are involved in NF-kappaB activation induced by the TNF-receptor, Edar and its adaptator Edaradd. Hum Mol Genet 14:3751-3757.

Nagarajan R, Le N, Mahoney H, Araki T, Milbrandt J (2002) Deciphering peripheral nerve myelination by using Schwann cell expression profiling. Proc Natl Acad Sci U S A 99:8998-9003.

Nave KA, Trapp BD (2008) Axon-glial signaling and the glial support of axon function. Annu Rev Neurosci 31:535-561.

Niimi T, Kumagai C, Okano M, Kitagawa Y (1997) Differentiation-dependent expression of laminin-8 (alpha 4 beta 1 gamma 1) mRNAs in mouse 3T3-L1 adipocytes. Matrix Biol 16:223-230.

Pan HC, Cheng FC, Chen CJ, Lai SZ, Lee CW, Yang DY, Chang MH, Ho SP (2007) Post-injury regeneration in rat sciatic nerve facilitated by neurotrophic factors secreted by amniotic fluid mesenchymal stem cells. J Clin Neurosci 14:1089-1098.

Pan W (2002) A comparative review of statistical methods for discovering differentially expressed genes in replicated microarray experiments. Bioinformatics 18:546-554.

Paradisi A, Maisse C, Bernet A, Coissieux MM, Maccarrone M, Scoazec JY, Mehlen P (2008a) NF-kappaB Regulates Netrin-1 Expression and Affects the Conditional Tumor Suppressive Activity of the Netrin-1 Receptors. Gastroenterology.

Paradisi A, Maisse C, Bernet A, Coissieux MM, Maccarrone M, Scoazec JY, Mehlen P (2008b) NF-kappaB regulates netrin-1 expression and affects the conditional tumor suppressive activity of the netrin-1 receptors. Gastroenterology 135:1248-1257.

Parman Y (2007) Hereditary neuropathies. Curr Opin Neurol 20:542-547.

Pereira RM, Calegari-Silva TC, Hernandez MO, Saliba AM, Redner P, Pessolani MC, Sarno EN, Sampaio EP, Lopes UG (2005) Mycobacterium leprae induces NF-kappaB-dependent transcription repression in human Schwann cells. Biochem Biophys Res Commun 335:20-26.

Perrier AL, Tabar V, Barberi T, Rubio ME, Bruses J, Topf N, Harrison NL, Studer L (2004) Derivation of midbrain dopamine neurons from human embryonic stem cells. Proceedings of the National Academy of Sciences of the United States of America 101:12543-12548.

Phulwani NK, Esen N, Syed MM, Kielian T (2008) TLR2 expression in astrocytes is induced by TNF-alpha- and NF-kappaB-dependent pathways. J Immunol 181:3841-3849.

Pittier R, Sauthier F, Hubbell JA, Hall H (2005) Neurite extension and in vitro myelination within three-dimensional modified fibrin matrices. J Neurobiol 63:1-14.

Prestori F, Rossi P, Bearzatto B, Laine J, Necchi D, Diwakar S, Schiffmann SN, Axelrad H, D'Angelo E (2008) Altered neuron excitability and synaptic plasticity in the cerebellar granular layer of juvenile prion protein knock-out mice with impaired motor control. J Neurosci 28:7091-7103.

Previtali SC, Nodari A, Taveggia C, Pardini C, Dina G, Villa A, Wrabetz L, Quattrini A, Feltri ML (2003) Expression of laminin receptors in schwann cell differentiation: evidence for distinct roles. J Neurosci 23:5520-5530.

Qin Y, Cheng C, Wang H, Shao X, Gao Y, Shen A (2008) TNF-alpha as an autocrine mediator and its role in the activation of Schwann cells. Neurochem Res 33:1077-1084.

Ravasz E, Somera AL, Mongru DA, Oltvai ZN, Barabasi AL (2002) Hierarchical organization of modularity in metabolic networks. Science 297:1551-1555.

Rodriguez AM, Pisani D, Dechesne CA, Turc-Carel C, Kurzenne JY, Wdziekonski B, Villageois A, Bagnis C, Breittmayer JP, Groux H, Ailhaud G, Dani C (2005) Transplantation of a multipotent cell population from human adipose tissue induces dystrophin expression in the immunocompetent mdx mouse. J Exp Med 201:1397-1405.

Ryu EJ, Yang M, Gustin JA, Chang LW, Freimuth RR, Nagarajan R, Milbrandt J (2008) Analysis of peripheral nerve expression profiles identifies a novel myelin glycoprotein, MP11. J Neurosci 28:7563-7573.

Rzhetsky A, Gomez SM (2001) Birth of scale-free molecular networks and the number of distinct DNA and protein domains per genome. Bioinformatics 17:988-996.

Sayyed-Ahmad A, Tuncay K, Ortoleva PJ (2007) Transcriptional regulatory network refinement and quantification through kinetic modeling, gene

expression microarray data and information theory. BMC Bioinformatics 8:20.

Schafers M, Brinkhoff J, Neukirchen S, Marziniak M, Sommer C (2001) Combined epineurial therapy with neutralizing antibodies to tumor necrosis factor-alpha and interleukin-1 receptor has an additive effect in reducing neuropathic pain in mice. Neurosci Lett 310:113-116.

Schneidman E, Berry MJ, 2nd, Segev R, Bialek W (2006) Weak pairwise correlations imply strongly correlated network states in a neural population. Nature 440:1007-1012.

Shannon CE (1997) The mathematical theory of communication. 1963. MD Comput 14:306-317.

Sharma S, Chopra K, Kulkarni SK (2007) Effect of insulin and its combination with resveratrol or curcumin in attenuation of diabetic neuropathic pain: participation of nitric oxide and TNF-alpha. Phytother Res 21:278-283.

Shibata T, Naruse K, Kamiya H, Kozakae M, Kondo M, Yasuda Y, Nakamura N, Ota K, Tosaki T, Matsuki T, Nakashima E, Hamada Y, Oiso Y, Nakamura J (2008) Transplantation of bone marrow-derived mesenchymal stem cells improves diabetic polyneuropathy in rats. Diabetes 57:3099-3107.

Shmulevich I, Dougherty ER, Kim S, Zhang W (2002) Probabilistic Boolean Networks: a rule-based uncertainty model for gene regulatory networks. Bioinformatics 18:261-274.

Sommer C, Schmidt C, George A (1998) Hyperalgesia in experimental neuropathy is dependent on the TNF receptor 1. Exp Neurol 151:138-142.

Sommer C, Lindenlaub T, Teuteberg P, Schafers M, Hartung T, Toyka KV (2001) Anti-TNF-neutralizing antibodies reduce pain-related behavior in two different mouse models of painful mononeuropathy. Brain Res 913:86-89.

Stellwagen D, Malenka RC (2006) Synaptic scaling mediated by glial TNF-alpha. Nature 440:1054-1059.

Stoll G, Muller HW (1999) Nerve injury, axonal degeneration and neural regeneration: basic insights. Brain Pathol 9:313-325.

Stoll G, Jung S, Jander S, van der Meide P, Hartung HP (1993) Tumor necrosis factor-alpha in immune-mediated demyelination and Wallerian degeneration of the rat peripheral nervous system. J Neuroimmunol 45:175-182.

Stubgen JP (2008) Tumor necrosis factor-alpha antagonists and neuropathy. Muscle Nerve 37:281-292.

Svenningsen AF, Shan WS, Colman DR, Pedraza L (2003) Rapid method for culturing embryonic neuron-glial cell cocultures. J Neurosci Res 72:565-573.

Takano K, Miki T, Katahira J, Yoneda Y (2007) NXF2 is involved in cytoplasmic mRNA dynamics through interactions with motor proteins. Nucleic Acids Res 35:2513-2521.

Taoufik E, Petit E, Divoux D, Tseveleki V, Mengozzi M, Roberts ML, Valable S, Ghezzi P, Quackenbush J, Brines M, Cerami A, Probert L (2008) TNF receptor I sensitizes neurons to erythropoietin- and VEGF-mediated neuroprotection after ischemic and excitotoxic injury. Proc Natl Acad Sci U S A 105:6185-6190.

Tegner J, Yeung MK, Hasty J, Collins JJ (2003) Reverse engineering gene networks: integrating genetic perturbations with dynamical modeling. Proc Natl Acad Sci U S A 100:5944-5949.

Tong AH et al. (2004) Global mapping of the yeast genetic interaction network. Science 303:808-813.

Tracey KJ (2002) The inflammatory reflex. Nature 420:853-859.

Tracey KJ, Fong Y, Hesse DG, Manogue KR, Lee AT, Kuo GC, Lowry SF, Cerami A (1987) Anti-cachectin/TNF monoclonal antibodies prevent septic shock during lethal bacteraemia. Nature 330:662-664.

Tracey KJ, Wei H, Manogue KR, Fong Y, Hesse DG, Nguyen HT, Kuo GC, Beutler B, Cotran RS, Cerami A, et al. (1988) Cachectin/tumor necrosis factor induces cachexia, anemia, and inflammation. J Exp Med 167:1211-1227.

Upadhyay G, Goessling W, North TE, Xavier R, Zon LI, Yajnik V (2008) Molecular association between beta-catenin degradation complex and Rac guanine exchange factor DOCK4 is essential for Wnt/beta-catenin signaling. Oncogene.

van Noort V, Snel B, Huynen MA (2004) The yeast coexpression network has a small-world, scale-free architecture and can be explained by a simple model. EMBO Rep 5:280-284.

Wagner R, Myers RR (1996) Endoneurial injection of TNF-alpha produces neuropathic pain behaviors. Neuroreport 7:2897-2901.

Webster HD (1993) Development of peripheral nerve fibers. In: In Peripheral Neuropathy (Dyck PJ, Thomas, P.K., Low P.A., and Poduslo. J.F., ed), pp 243-266. Philadelphia: W.B. Saunders.

Weiss MD, Luciano CA, Quarles RH (2001) Nerve conduction abnormalities in aging mice deficient for myelin-associated glycoprotein. Muscle Nerve 24:1380-1387.

Yang LY, Liu XM, Sun B, Hui GZ, Fei J, Guo LH (2004) Adipose tissue-derived stromal cells express neuronal phenotypes. Chin Med J (Engl) 117:425-429.

Yarwood SJ, Woodgett JR (2001) Extracellular matrix composition determines the transcriptional response to epidermal growth factor receptor activation. Proc Natl Acad Sci U S A 98:4472-4477.

Yeung N, Cline MS, Kuchinsky A, Smoot ME, Bader GD (2008) Exploring biological networks with Cytoscape software. Curr Protoc Bioinformatics Chapter 8:Unit 8 13.

Yu WM, Yu H, Chen ZL (2007) Laminins in peripheral nerve development and muscular dystrophy. Molecular neurobiology 35:288-297.

Yu WM, Feltri ML, Wrabetz L, Strickland S, Chen ZL (2005) Schwann cell-specific ablation of laminin gamma1 causes apoptosis and prevents proliferation. J Neurosci 25:4463-4472.

Zhang Y, Andl T, Yang SH, Teta M, Liu F, Seykora JT, Tobias JW, Piccolo S, Schmidt-Ullrich R, Nagy A, Taketo MM, Dlugosz AA, Millar SE (2008)

Activation of beta-catenin signaling programs embryonic epidermis to hair follicle fate. Development 135:2161-2172.